

ELECTRONIC SUPPLEMENTARY INFORMATION FOR:

A precise and versatile platform for rapid glycosylation analysis of brain tissue

Mattia Vacchini, Laura Cipolla, Olga Gornik, Gordan Lauc and Thomas Klarić

TABLE OF CONTENTS:

Table ST-1. Validation parameters of LSD in comparison to related N-glycomic workflows in the literature.

Figure S-1. HSD and $LSD^{mg/\mu L}$ N-glycan extraction and 2-AB N-glycan labelling.

Figure S-2. HSD and $LSD^{mg/\mu L}$ linearity analysis.

Figure S-3. $LSD^{\mu L}$ specificity and carryover effect.

Figure S-4. Amount-dependent variation in the chromatographic profile of brain tissue samples analysed by HSD.

Figure S-5. Chromatograms of brain samples analysed by LSD^{mg} are consistent regardless of starting tissue amount.

Figure S-6. Chromatograms of brain samples analysed by $LSD^{\mu L}$ are consistent regardless of starting tissue amount.

Figure S-7. Similarity of profiles obtained by $LSD^{\mu L}$ and LSD^{mg} .

Figure S-8. Adding a second round of N-glycan extraction has little effect on the chromatographic profile of brain samples analysed by $LSD^{\mu L}$ even when the polarity of the aqueous phase is changed.

Figure S-9. Stability of samples stored in lysis buffer.

Figure S-10. A single overnight deglycosylation step is insufficient for complete N-glycan release.

Figure S-11. The LSD lysate is compatible with downstream proteomics applications.

Figure S-12. $LSD^{\mu L}$ sensitivity increases 10-fold when N-glycans are labelled with Procainamide.

Figure S-13. Elution trend of the N-glycans and external standard monoisotopic masses.

Table ST-2. Mass spectrometry analyses of LSD and HSD chromatographic profiles.

Table ST-3. Examples of glycoproteins identified by downstream proteomics applications using the LSD lysate.

Figure S-14. LSD and HSD structural resolution on each starting brain tissue amount.

Figure S-15. Comparison of HSD and $LSD^{\mu L}$ chromatographic profiles.

Figure S-16. Chromatographic sections whose abundance is significantly different between methods by N-glycan type.

Figure S-17. MS spectra extracts exemplifying monosaccharide compositions uniquely identified by the LSD method.

Figure S-18. Derived traits: grouping of N-glycans according to structural features for each method.

Supplementary material 1: Calculation of derived traits.

Supplementary material 2: Detailed LSD protocol

N-glycoanalytical workflow reference (Ref. n°)	Starting amount of brain tissue (mg)	Sample prep. (days)	Sensitivity	Precision (i.e., CV%, PCC)	Robustness	Linearity	Range (mg)	Selectivity
<i>Glycoconj. J.</i> , 1992, 9 , 293–301. (6)	6000	> 3	✗	✗	✗	✗	✗	✗
<i>Eur. J. Biochem.</i> , 1998, 251 , 691–703. (7)	6000	> 3	✗	✗	✗	✗	✗	✗
<i>Eur. J. Biochem.</i> , 1998, 258 , 243–270. (8)	6000	> 3	✗	✗	✗	✗	✗	✗
<i>Glycobiology</i> , 2007, 17 , 261–276. (9)	2	?	✗	✗	✗	✗	✗	✗
<i>J. Neurochem.</i> , 2007, 103 , 25–31. (10)	> 3000	?	✗	✗	✗	✗	✗	✗
<i>Anal. Biochem.</i> , 2012, 423 , 253–260. (11)	?	?	✗	✗	✗	✗	✗	✗
<i>Anal. Chem.</i> , 2013, 85 , 4074–4079. (19)	< 0.001	< 3 (hours)	✗	CV 35%	✗	✗	✗	✗
<i>J. Proteome Res.</i> , 2013, 12 , 5791–5800. (12)	?	≥ 3	✗	✗	✗	✗	✗	✗
<i>Glycoconj. J.</i> , 2014, 31 , 671–683 (13)	2	?	✗	✗	✗	✗	✗	✗
<i>Biochim. Biophys. Acta</i> , 2015, 1850 , 1704–1718. (14)	?	≥ 3	✗	✗	✗	✗	✗	✗
<i>Anal. Chem.</i> , 2015, 87 , 2869–2877. (15)	1.5	≥ 3	✓	PCC > 0.98	✗	✗	✗	✗
<i>Biochim. Biophys. Acta</i> , 2016, 1860 , 1716–27. (16)	> 1000	≥ 3	✗	✗	✗	✗	✗	✗
<i>Mol. Cell. Proteomics</i> , 2017, 16 , 2268–2280. (17)	?	≥ 3	✗	✗	✗	✗	✗	✗
<i>High-Throughput Glycomics and Glycoproteomics</i> , Humana Press, New York, NY, 2017, pp. 207–216. (18)	25	≥ 3	✗	CV 4%	✗	✗	✗	✗
The LSD workflow presented in this work	1	3	✓	CV 6%	✓	R ² = 0.9961	1-10	✓

Table ST-1. Validation parameters of LSD in comparison to similar N-glycomic workflows in the literature. Parameters considered in this table are relative to the analysis of N-glycans from brain tissue samples. Method validation carried out on different samples (i.e., cell lysate, plasma, isolated N-glycoproteins) within papers also analysing brain N-glycans is not considered: a validated method is not transferable between different kind of samples, unless evidence of its transferability is provided. Starting amount of brain tissue = mgs of fresh biological material entering the workflow; Sample prep. (days) = approximated value based on available information (i.e., available timings in the experimental section); Sensitivity = does the considered work contain any testing

of the method sensitivity (i.e., slope of the calibration curve, normalized intensity of the signals at different sample concentrations)?; Precision = does the considered work contain any testing (i.e., CV%, PCC) of the method precision?; Robustness = was the capacity of the method to remain unaffected by small, but deliberate variations in its parameters tested?; Linearity = was the method tested on different amounts of starting material? Was the linearity assessed by giving, at least, an R² value?; Range = does the considered work specify a range of sample amount on which the method's performance is reliable (i.e., precise, sensitive)?; Selectivity = was the method tested for its selectivity towards the desired analyte? Red-crossed cells = no data; Orange cells with question mark = not stated clearly / difficult to be inferred; CV = coefficient of variation; PCC = Pearson correlation coefficient.

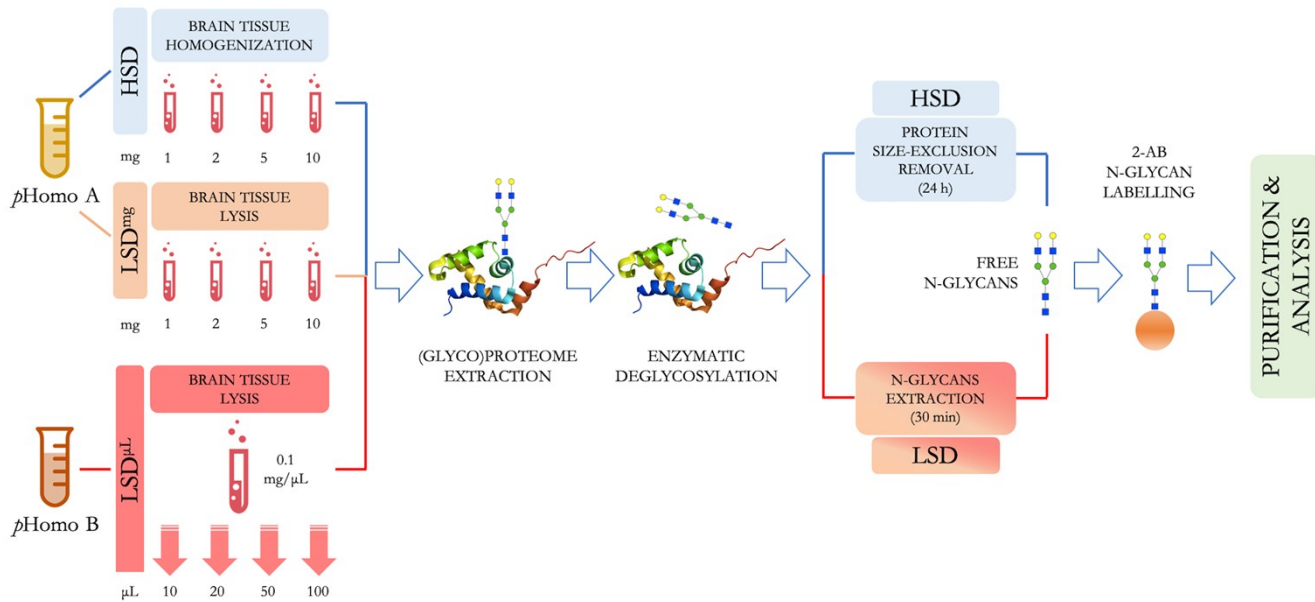


Figure S-1. HSD and LSD^{mg/μL} N-glycan extraction and 2-AB N-glycan labelling. Purification & analysis include GHP for HILIC-UPLC-FLR and GHP followed by PGC-SPE for HILIC-UPLC-ESI-QqTOF-MS.

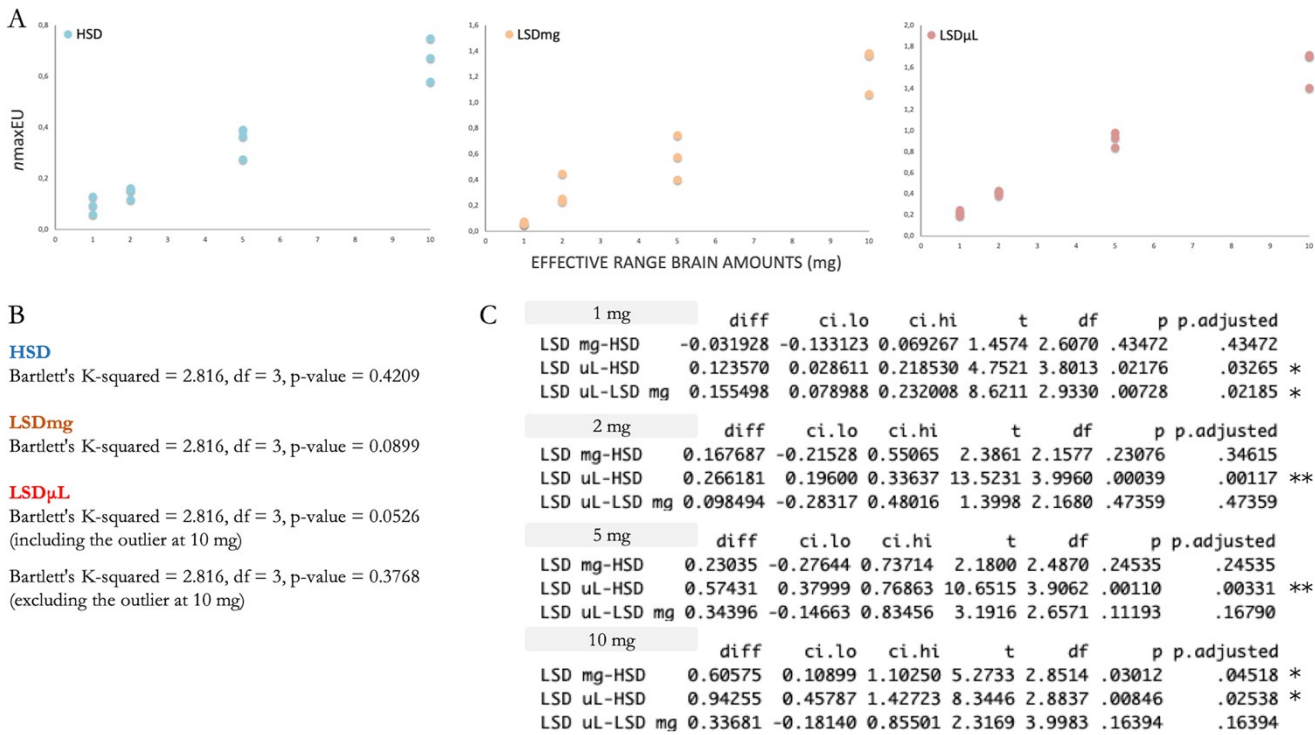


Figure S-2. HSD and LSD^{mg/μL} linearity analysis. **A.** Scatter plots for a visual analysis of the variance of replicates for each starting amount of brain tissue in the effective range. **B.** Bartlett's test of homogeneity of variances: the test null-hypothesis is that all the replicates have the same variance. **C.** Statistical significance (Welch's ANOVA, Games-Howell post-hoc test) of the differences in nmaxEU between methods for each starting amount of brain tissue in the effective range (n=1, triplicates, *p < 0.05, ** p < 0.01).

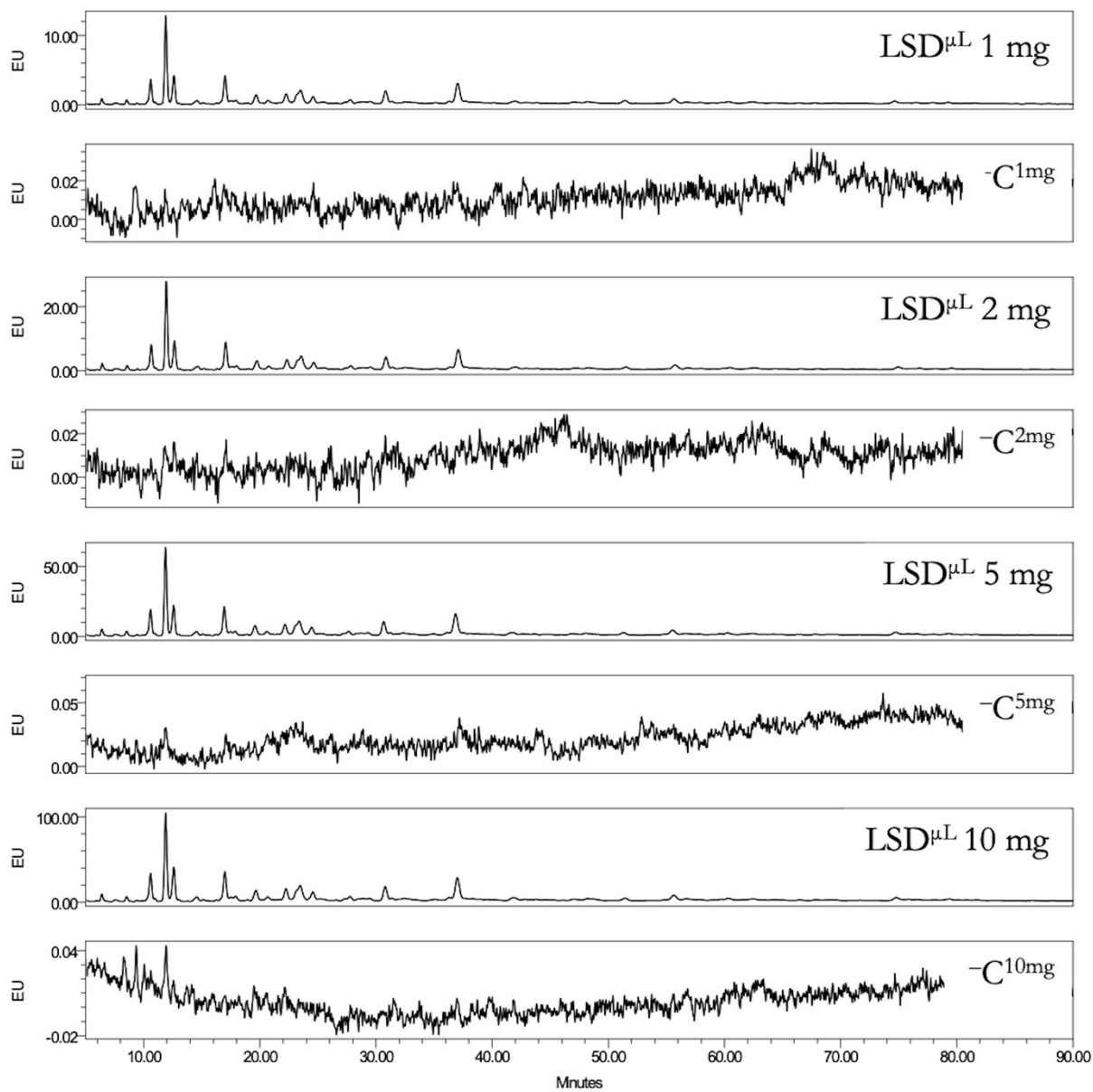


Figure S-3. $\text{LSD}^{\mu\text{L}}$ specificity and carryover effect. Chromatograms of labelled and unlabeled (${}^1\text{C}$) samples are shown for each starting amount of brain tissue in the effective range.

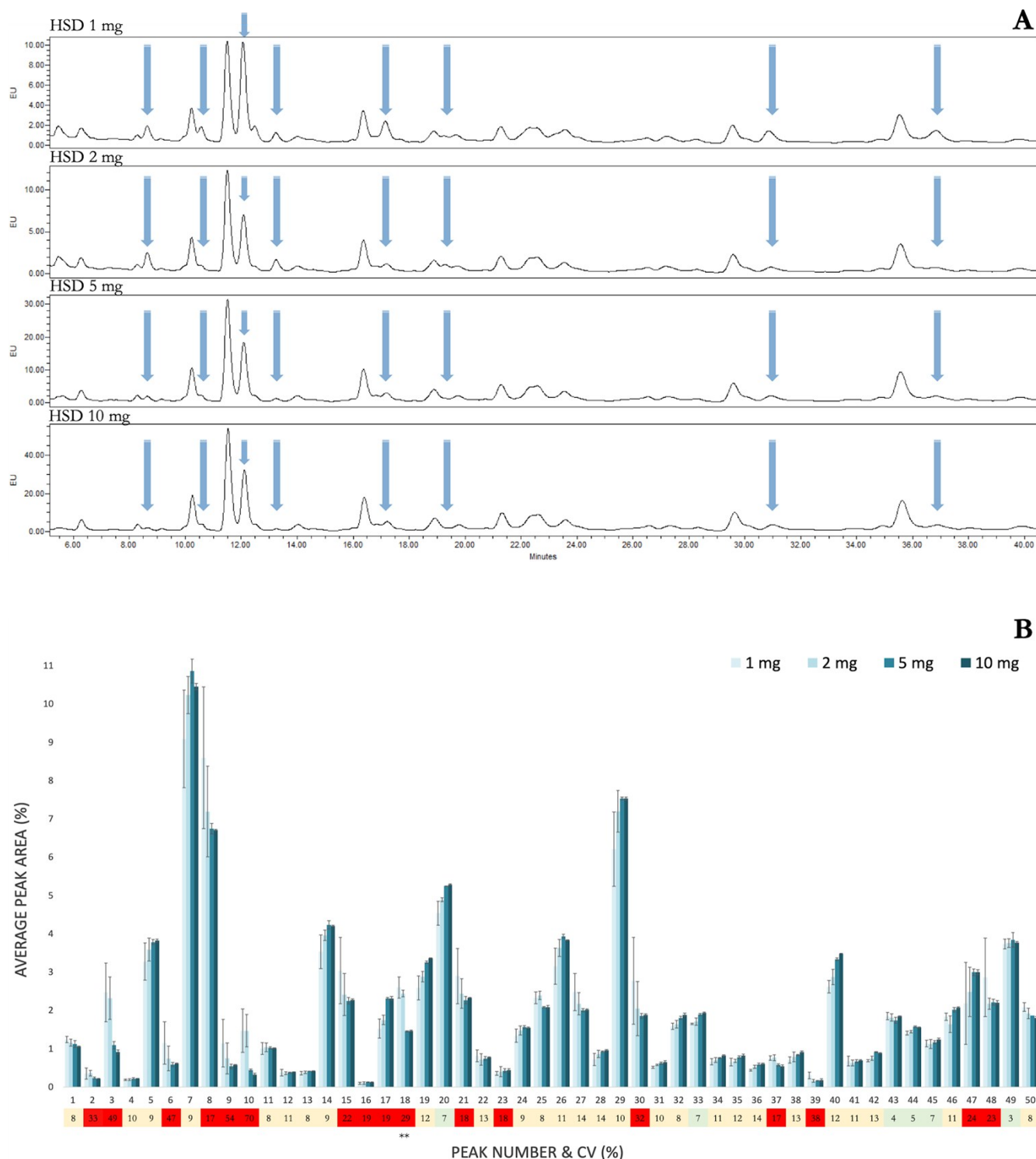


Figure S-4. Amount-dependent variation in the chromatographic profile of brain tissue samples analysed by HSD. **A.** Qualitative comparison of HSD chromatograms in the effective range of starting brain tissue amounts. Chromatograms are cut at 41 min to better highlight examples of varying chromatographic sections. Arrows indicate variable chromatographic sections. **B.** Quantitative comparison of HSD chromatograms in the effective range of starting brain tissue amounts. Descriptive error bars show data spread within replicates ($n = 1$, triplicates) as \pm SD. The CV for each chromatographic section is reported as a measure of precision of the value of the section area between different brain amounts (green = $CV \leq 7\%$; yellow = $7\% < CV \leq 15\%$; red = $CV > 15\%$). See Figure 2 for integration boundaries. Statistical significance of the differences (1 mg and/or 2 mg Vs 10 mg, Welch's ANOVA, Games-Howell post-hoc test) regarding chromatographic sections with CVs $> 15\%$ is reported (** $p < 0.01$).

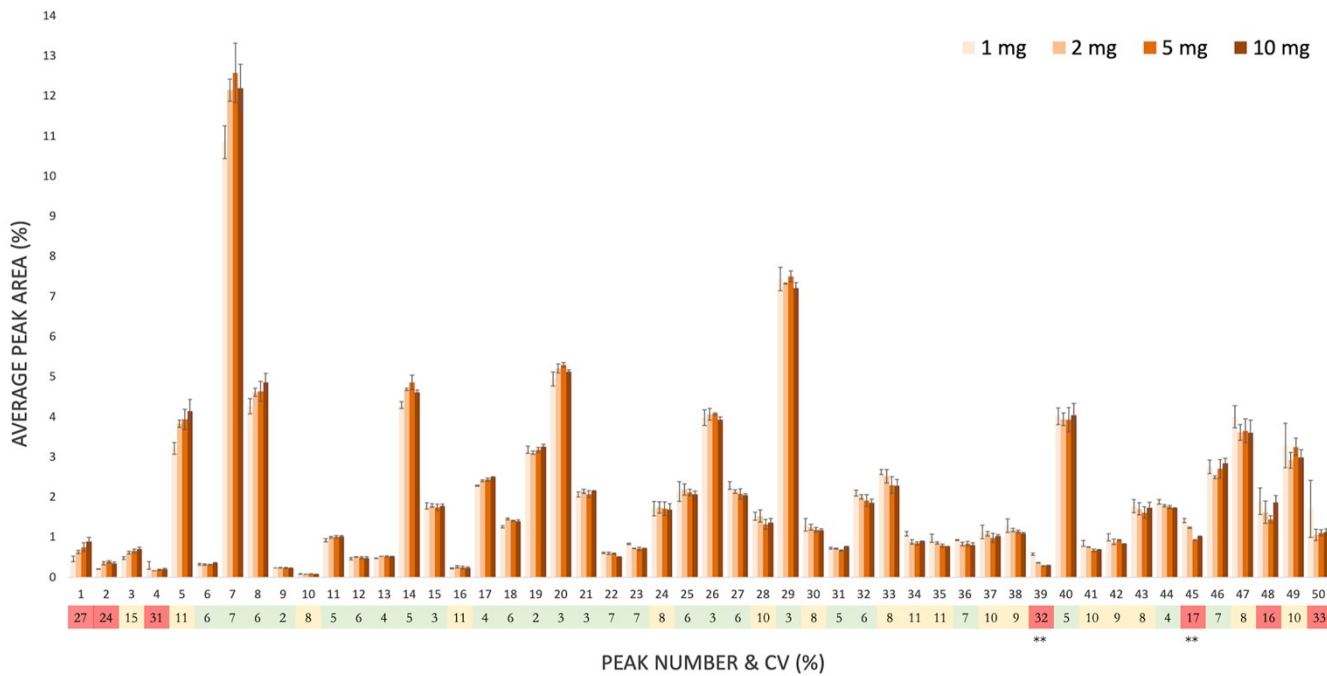
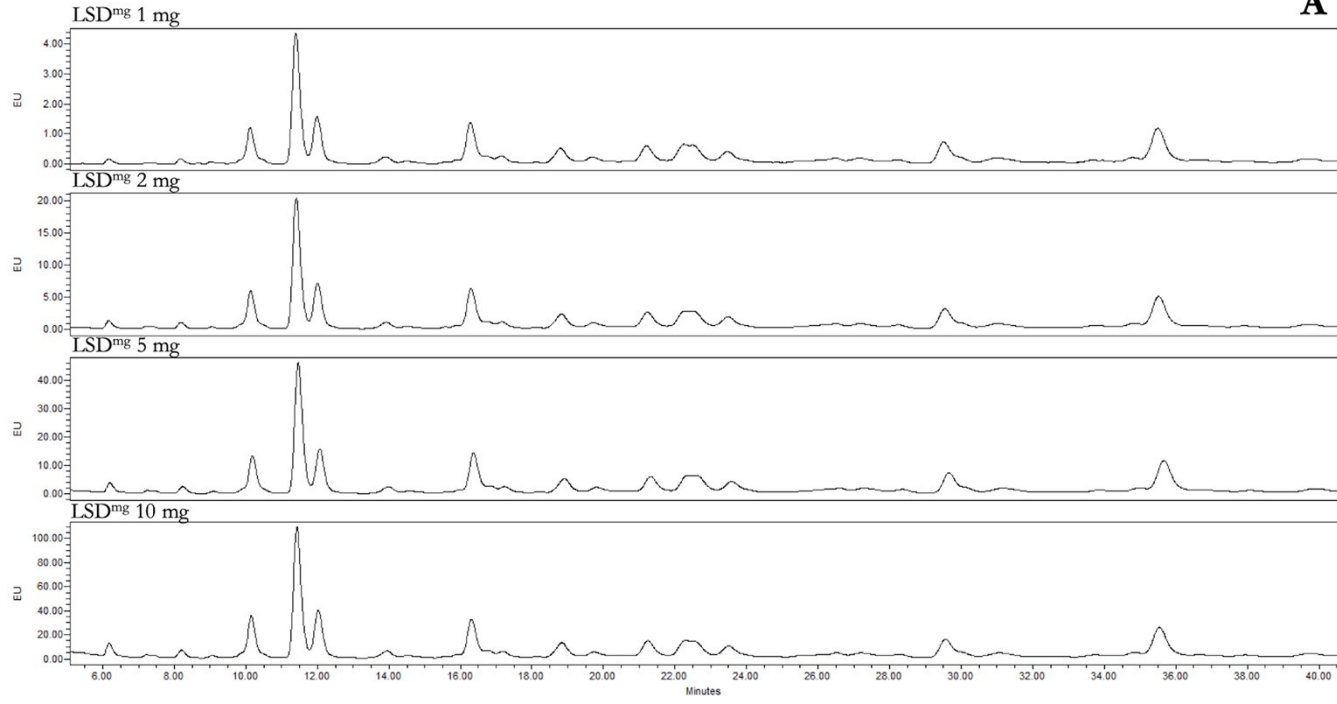
A

Figure S-5. Chromatograms of brain samples analysed by LSD^{mg} are more consistent regardless of starting tissue amount. **A.** Qualitative comparison of LSD^{mg} chromatograms in the effective range of starting brain tissue amounts. Chromatograms are cut at 41 min to highlight the same region considered in Figure S-4. **B.** Quantitative comparison of LSD^{mg} chromatograms in the effective range of starting brain tissue amounts. Descriptive error bars show data spread within replicates ($n = 1$, triplicates) as \pm SD. CV for each chromatographic section is reported as a measure of precision of the value of the same section area between different brain amounts (green = $CV \leq 7\%$; yellow = $7\% < CV \leq 15\%$; red = $CV > 15\%$). See Figure 2 for integration boundaries. Statistical significance of the differences (1 mg and/or 2 mg Vs 10 mg, Welch's ANOVA, Games-Howell post-hoc test) regarding chromatographic sections with CVs $> 15\%$ is reported (** $p < 0.01$).

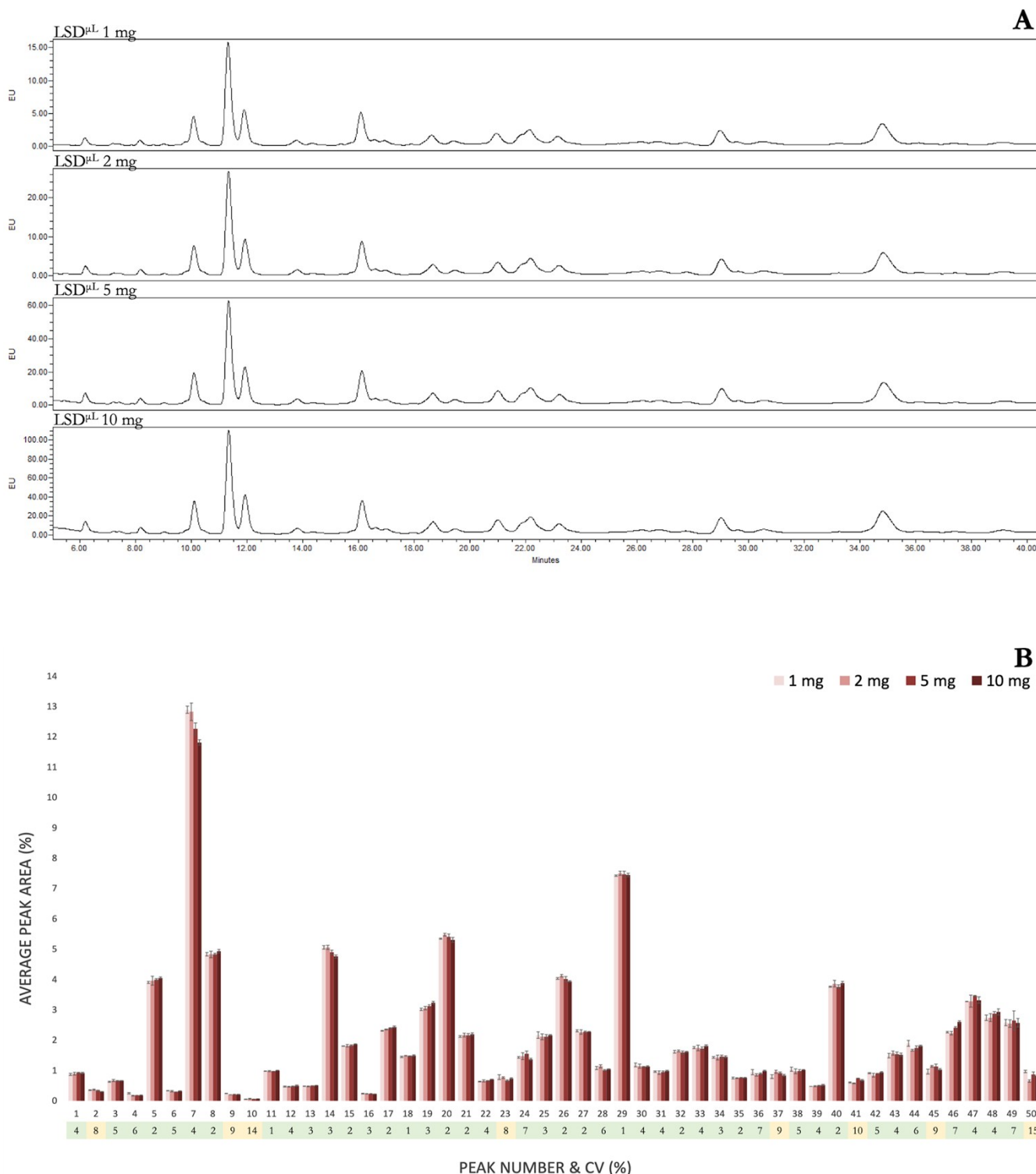


Figure S-6. Chromatograms of brain samples analysed by $\text{LSD}^{\mu\text{L}}$ are consistent regardless of starting tissue amount. **A.** Qualitative comparison of $\text{LSD}^{\mu\text{L}}$ chromatograms in the effective range of starting brain tissue amounts. Chromatograms are cut at 41 min to highlight the same region considered in Figures S-4/5. **B.** Quantitative comparison of $\text{LSD}^{\mu\text{L}}$ chromatograms in the effective range of starting brain tissue amounts. Descriptive error bars show data spread within replicates ($n = 1$, triplicates) as $\pm \text{SD}$. CV for each chromatographic section is reported as a measure of precision of the value of the same section area between different brain amounts (green = $\text{CV} \leq 7\%$; yellow = $7\% < \text{CV} \leq 15\%$; red = $\text{CV} > 15\%$). See Figure 2 for integration boundaries.

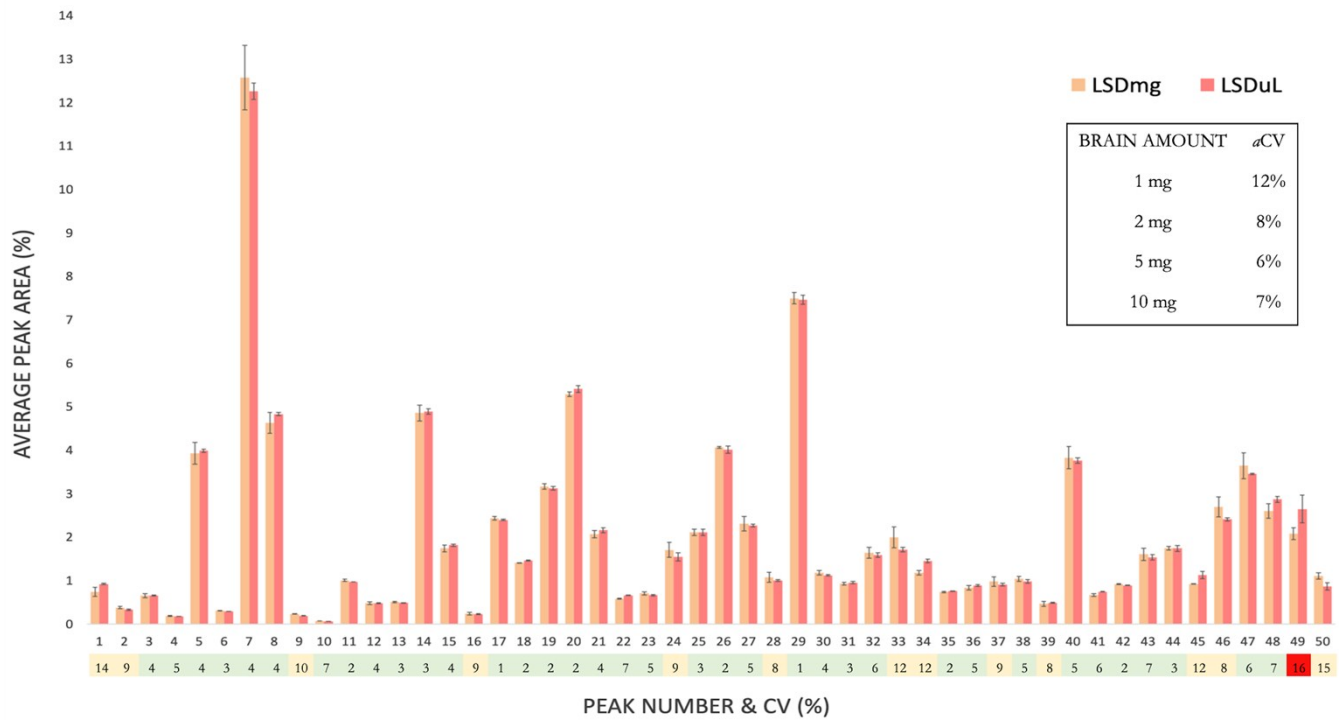


Figure S-7. Similarity of profiles obtained by $LSD^{\mu L}$ and LSD^{mg} . Quantitative comparison of $LSD^{\mu L}$ and LSD^{mg} chromatograms in the effective range of starting brain tissue amounts (5 mg profiles, representing the optimal brain amount, are displayed as an example). CV for each chromatographic section is reported as a measure of precision of the same section area between the two versions of the LSD method (green = $CV \leq 7\%$; yellow = $7\% < CV \leq 15\%$; red = $CV > 15\%$). No statistical significance ($LSD^{\mu L}$ 30.08 Vs $LSD^{\mu L}$ 31.07, $n=1$, triplicates, Wilcoxon-Mann-Whitney) was found for the differences in chromatographic sections with $CVs > 15\%$. α CVs for each starting amount of brain tissue within the effective range, calculated between the two LSD versions, are reported in the inset.

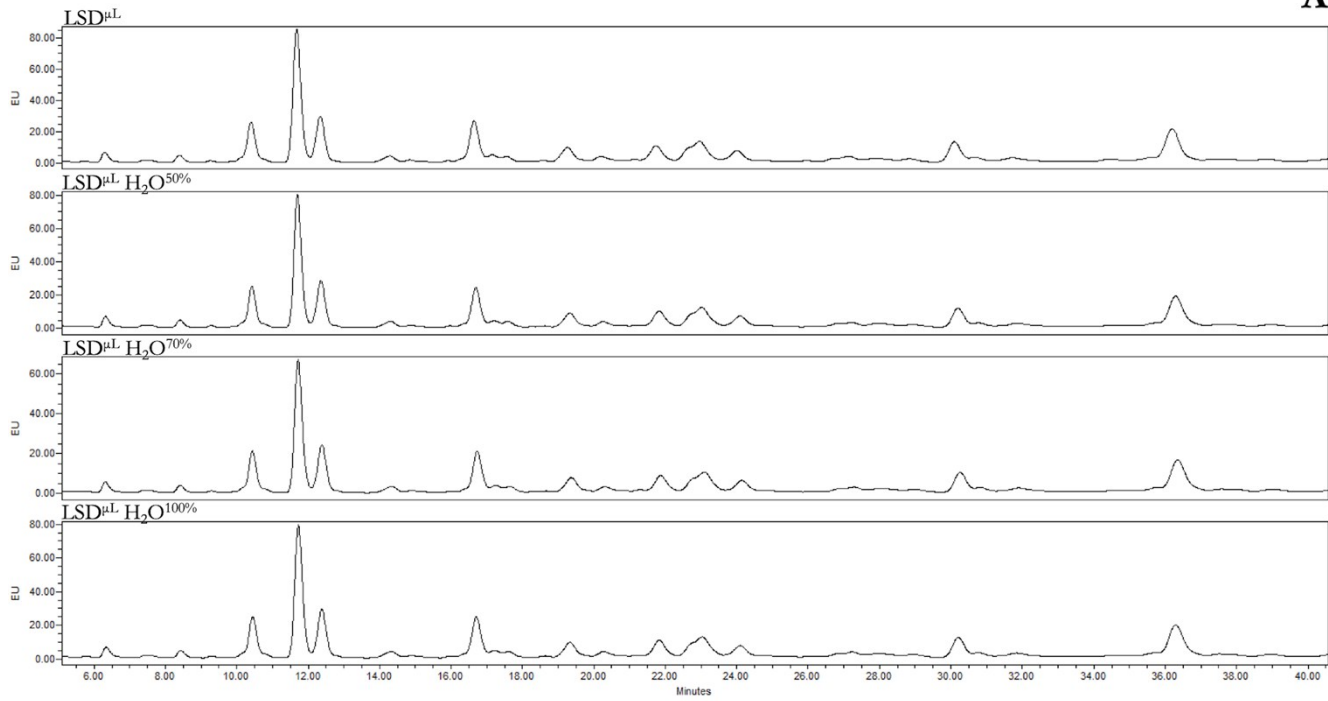
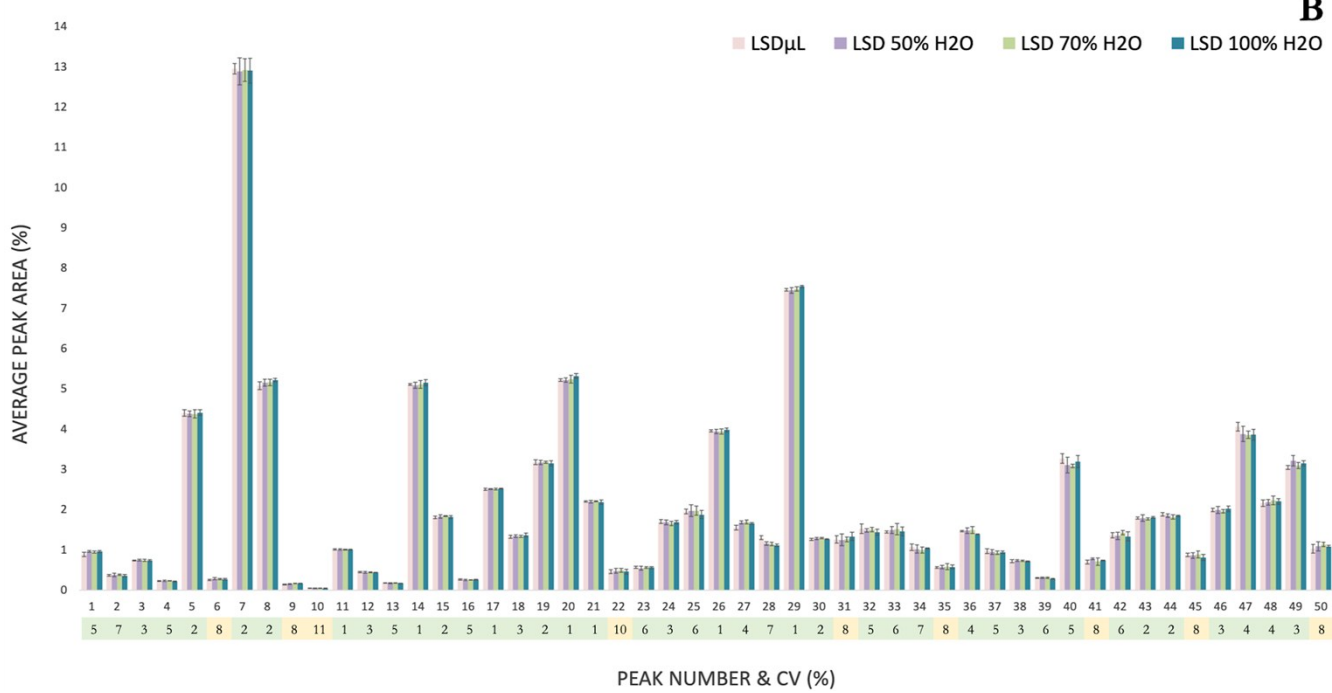
A**B**

Figure S-8. Adding a second round of N-glycan extraction has little effect on the chromatographic profile of brain samples analysed by LSD μ L even when the polarity of the aqueous phase is changed. **A.** Qualitative comparison of LSD μ L chromatograms obtained with a second round of N-glycan extraction, using aqueous phases of varying polarity. Chromatograms are cut at 41 min to better highlight the qualitative consistency of the profiles. **B.** Quantitative comparison of LSD μ L chromatograms obtained with the second round of N-glycan extraction with increasing polarity of the aqueous phase (% of H₂O reported in the legend refers to the second N-glycan extraction round; LSD μ L was performed with a single extraction step). Descriptive error bars show data spread within replicates ($n = 1$, triplicates) as \pm SD. CV for each chromatographic section is reported as a measure of precision of the value of the same section area amongst different aqueous phase polarities (green = CV \leq 7%; yellow = 7% $<$ CV \leq 15%; red = CV $>$ 15%). See Figure 2 for integration boundaries.

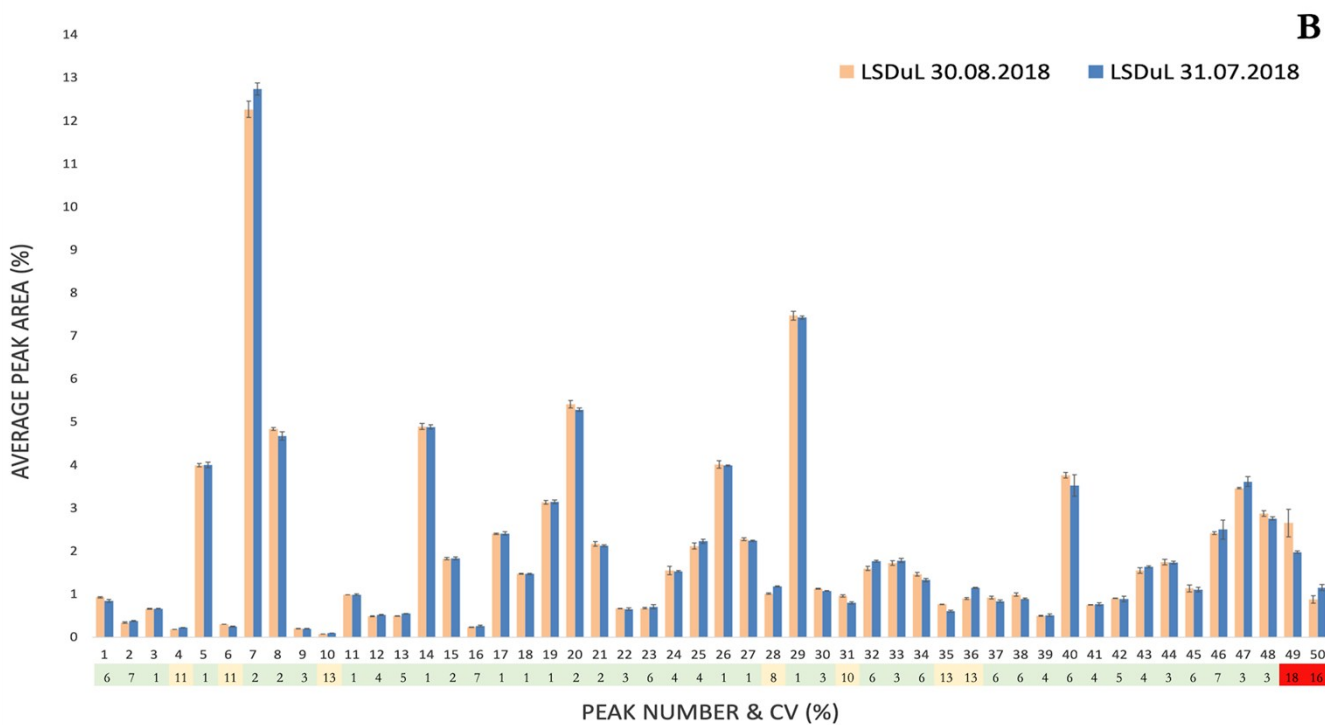
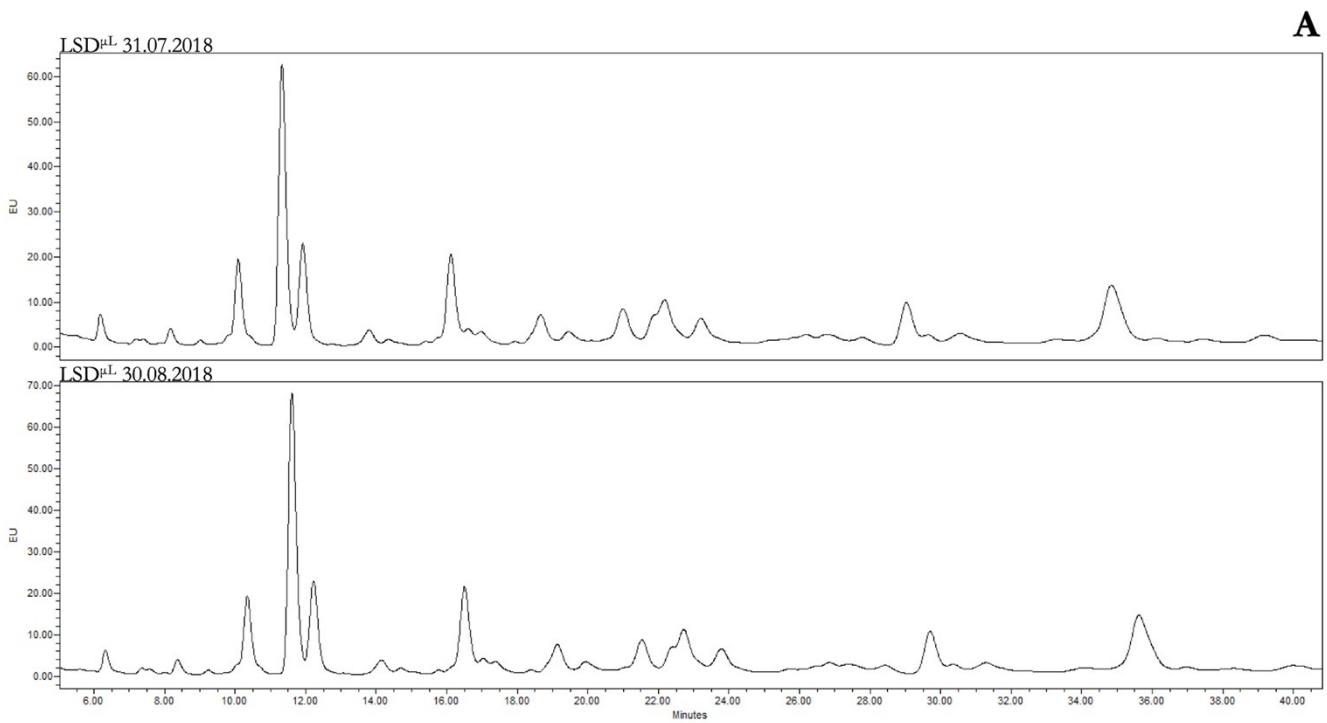


Figure S-9. Stability of samples stored in lysis buffer. N-glycome analysis by LSD μ L was performed on the same brain tissue lysate, frozen-thawed multiple times over a period of one month. **A.** Qualitative comparison of LSD μ L chromatograms in the aforementioned conditions. Chromatograms are cut at 41 min to be consistent with previously displayed sections. **B.** Quantitative comparison of LSD μ L chromatograms in the aforementioned conditions. Descriptive error bars show data spread within replicates ($n = 1$, triplicates) as \pm SD. CV for each chromatographic section is reported as a measure of precision of the same section area between the two experiments (green = CV \leq 7%; yellow = 7% $<$ CV \leq 15%; red = CV $>$ 15%). See Figure 2 for integration boundaries. No statistical significance (LSD μ L 30.08 Vs LSD μ L 31.07, $n=1$, triplicates, Wilcoxon signed-rank test) was found for the differences in chromatographic sections with CVs $>$ 15%.

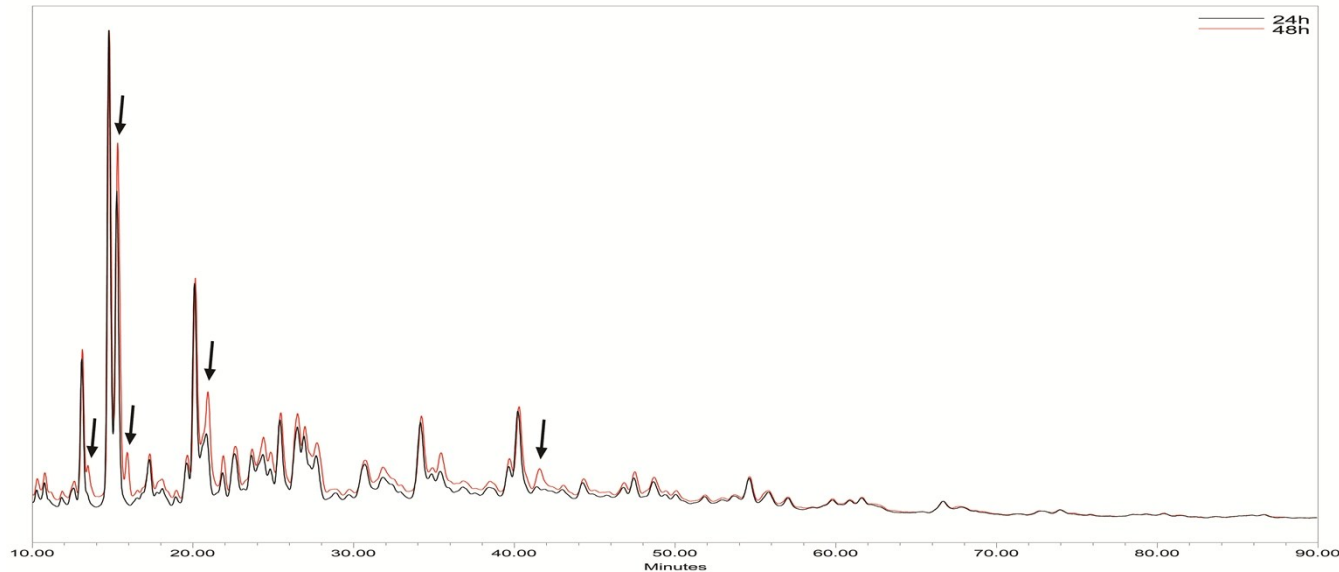


Figure S-10. A single overnight deglycosylation step is insufficient for complete N-glycan release. LSD was employed on identical aliquots of the same brain lysate using either a single overnight deglycosylation step (black chromatogram) or an overnight deglycosylation followed by the addition of more PNGase F with further incubation overnight (red chromatogram) and the resulting N-glycosylation profiles were analysed by UPLC and compared. Two consecutive overnight incubations resulted in a substantial increase in the relative abundance of several chromatographic peaks as well as the appearance of two previously undetectable peaks (arrows). Representative chromatograms are shown ($n=3$ per condition).

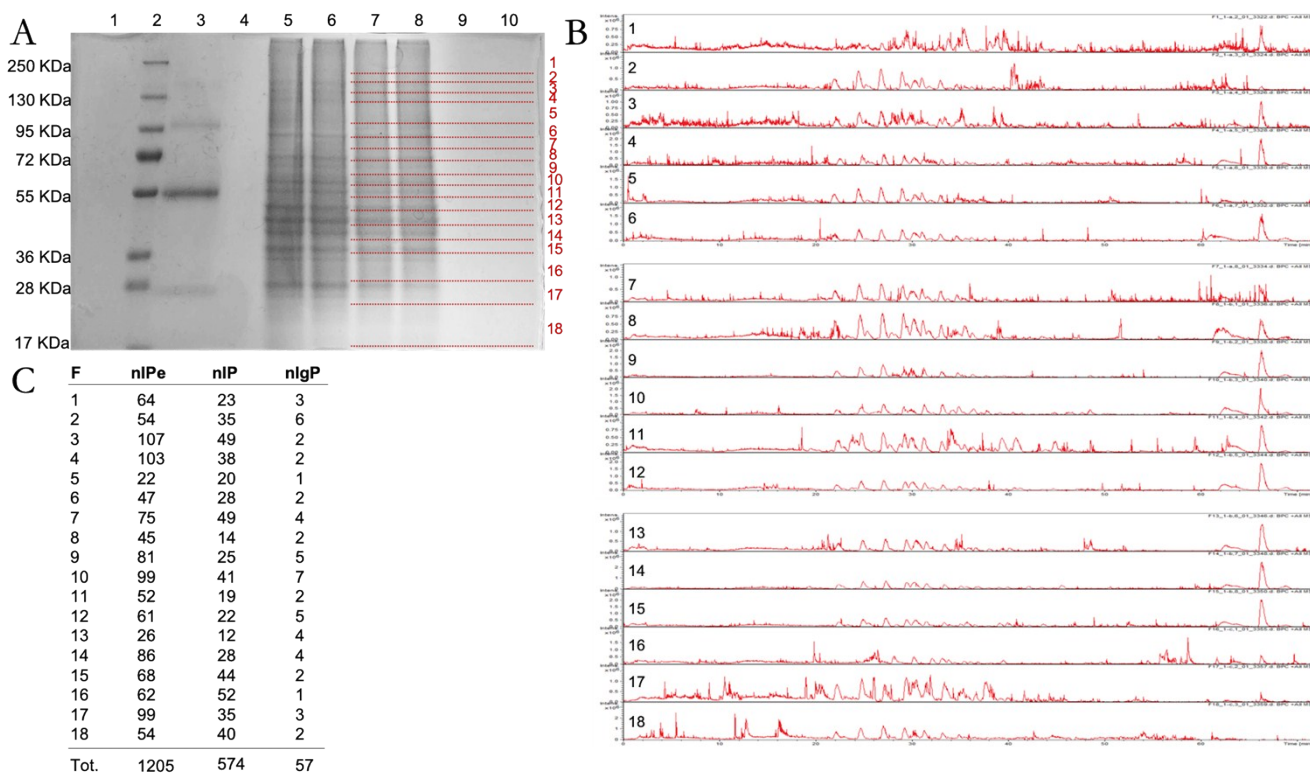


Figure S-11. The LSD lysate is compatible with downstream proteomics applications. **A.** SDS-PAGE of the reduced, denatured and alkylated lysate. 1,4,9,10 = blanks; 2 = molecular weight marker; 3 = human IgG as positive control; 5,6,7,8 = brain tissue lysate; left legend = molecular weights of the marker; right legend (red) = fractionation pattern (18 fractions). **B.** LC-MS BPC spectra of deglycosylated peptides obtained from the 18 fractions excised from the SDS-PAGE. **C.** Number of identified peptides and proteins obtained from the 18 fractions excised from the SDS-PAGE. F = fraction; nIPe = n° of identified peptides in each fraction; nIP = n° of identified proteins in each fraction; nlgP = n° of putative glycoproteins identified in each fraction (at least one Asn→Asp, +0.984 Da; detailed examples of identified glycoproteins are given in Table ST-3).

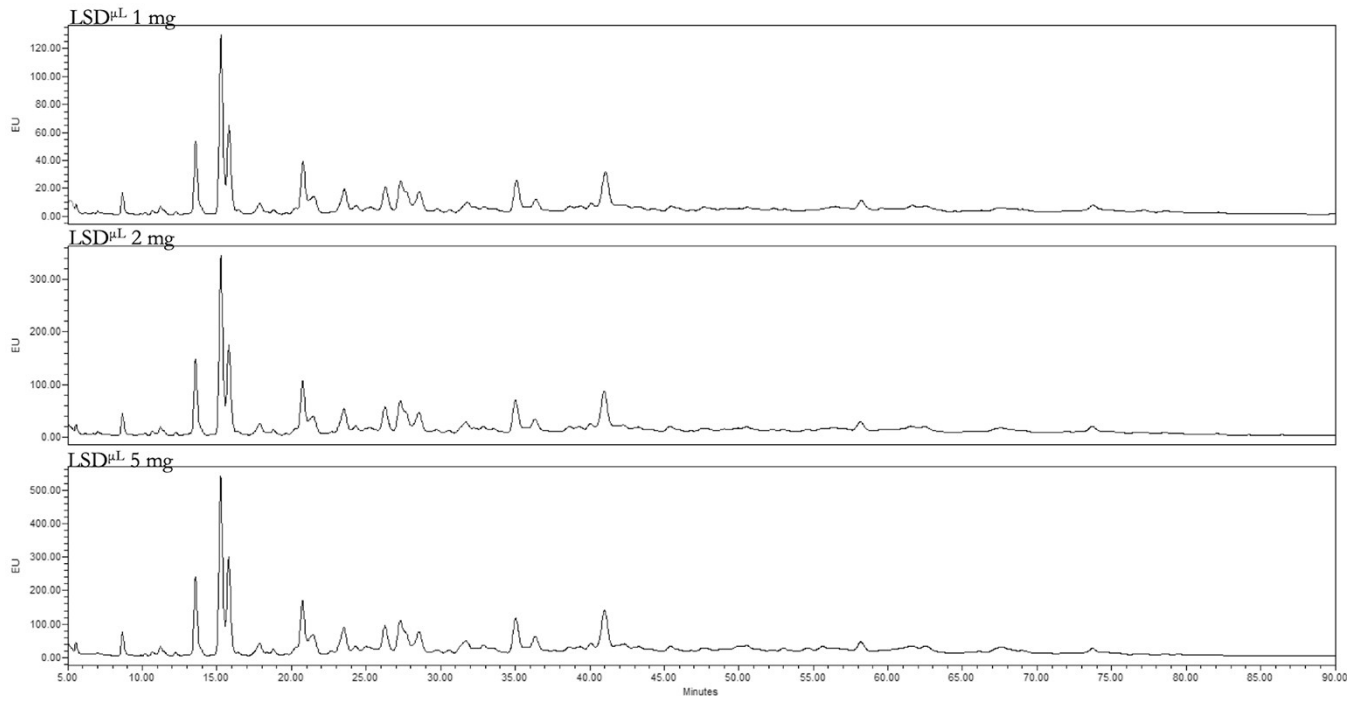


Figure S-12. LSD μ L sensitivity increases 10-fold when N-glycans are labelled with Procainamide instead of 2-AB. 1, 2 and 5 mg profiles are reported as examples. Note the signal intensity on the y-axis.

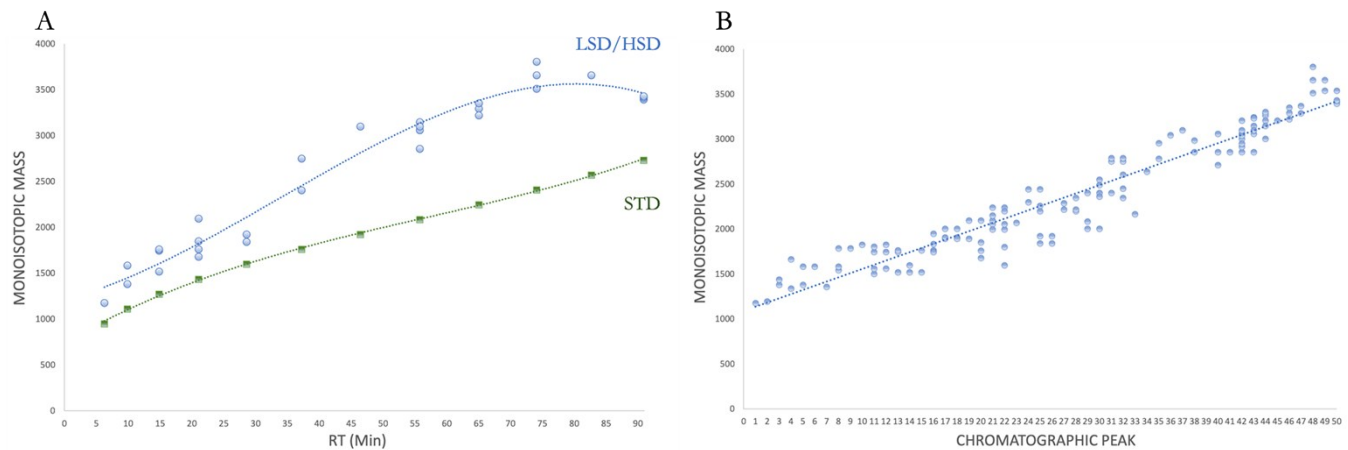
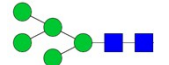
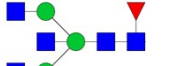
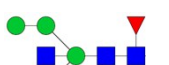
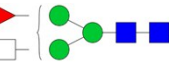
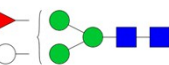
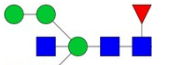
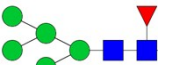
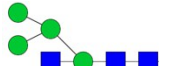


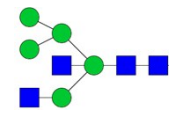
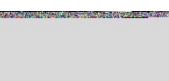
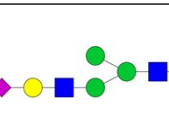
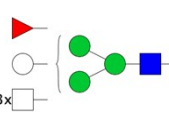
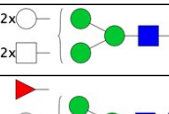
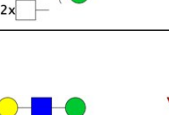
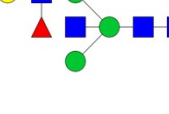
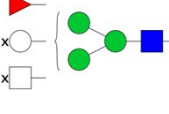
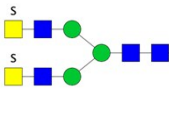
Figure S-13. Elution trend of the extracted brain N-glycans and external standard by monoisotopic mass. **A.** Comparison of the elution trend of the LSD/HSD N-glycan monoisotopic masses (blue) and the external standard of 2-AB labeled hydrolyzed glucose oligomers masses (STD, green). **B.** LSD/HSD monoisotopic masses eluting in each chromatographic section.

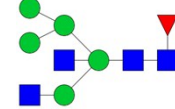
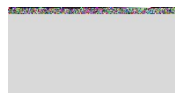
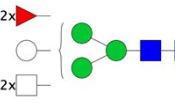
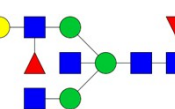
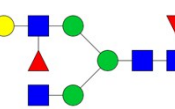
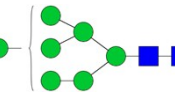
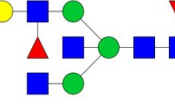
Table ST-2. Mass spectrometry analyses of LSD and HSD chromatographic profiles.

CS	GS	MMM (u)	TUM (u)	MFM (u)	TLM (u)	RMA (ppm)	MC	MS ²	DFI	PGS
1		1177.4552	1056.3857	1056.3786	1177.4622	6.0	H3N2F1	Y	1177 (Int); 1031 (-F); 1015 (-H); 869 (-F -H); 853 (-2H); 707 (-F -2H); 545 (2N2AB); 528 (2HN); 488 (NF2AB, CF); 366 (HN); 342 (N2AB); 325 (2H)	
2		1193.4505	1072.3806	1072.3739	1193.4571	5.6	H4N2	Y	1193 (Int); 1031 (-H); 869 (-2H); 852 (-N2AB); 707 (-3H); 545 (-4H); 528 (2HN); 366 (HN); 342 (N2AB); 325 (2H)	
3	A	1380.5321	1259.4651	1259.4555	1380.5416	6.9	H3N3F1	Y	1380 (Int); 1234 (-F); 1218 (-H); 1177 (-N, CF); 1072 (-F -H); 1031 (-FN); 1015 (-H -N); 910 (H3N2AB, Bis); 853 (-2H -N); 569 (2NH/Bis?); 488 (NF2AB, CF); 366 (HN); 342 (N2AB); 325 (2H)	
	B	1437.5527	1316.4866	1316.4761	1437.5631	7.3	H3N4	Y	1437 (Int); 1234 (-N); 1096 (-N2AB); 1072 (-H - N); 1031 (-2N); 910 (H3N2AB, Bis); 893 (3H2N); 869 (-2N -H); 707 (-2N -2H); 569 (2NH/Bis?); 545 (2N2AB); 528 (2HN); 366 (HN); 342 (N2AB); 325 (2H)	
4	A	1339.5072	1218.4385	1218.4306	1339.5150	5.8	H4N2F1	Y	1339 (Int); 1193 (-F); 1177 (-H, CF); 1031 (-F -H); 1031 (-HF); 1015 (-2H); 869 (-2H -F); 707 (-3H -F); 488 (NF2AB, CF); 545 (2N2AB); 528 (2HN); 366 (HN); 342 (N2AB); 325 (2H)	
	B	1663.5633	1542.5013	1542.4867	1663.5778	8.7	H3N4F1Su1	N		
5	A	1583.6068	1462.5445	1462.53023	1583.6210	9.0	H3N4F1	Y	1583 (Int); 1437 (-F); 1380 (-N); 1234 (-N -F); 1218 (-N -H); 1177 (-2N, CF); 1056 (-N - 2H , Bis + CF); 1072 (-N -H -F); 1015 (-2N -H); 910 (H3N2AB, Bis); 853 (-2N -2H); 707 (-2N -2H -F); 691 (-2N -3H, CF); 569 (2NH/Bis?); 488 (NF2AB, CF); 545 (2N2AB); 528 (2HN); 366 (HN); 342 (N2AB); 325 (2H)	
	B	1380.5311	1259.4651	1259.45453	1380.5416	7.6	H3N3F1	N		
6		1583.608	1462.5445	1462.53143	1583.6210	8.2	H3N4F1	N		

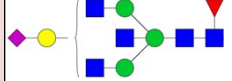
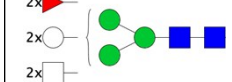
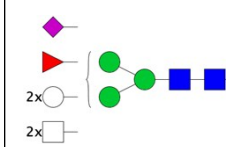
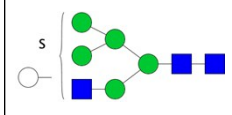
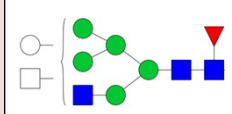
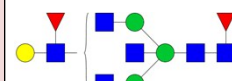
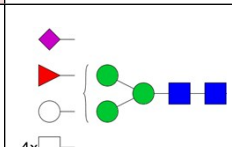
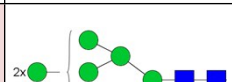
7		1355.5002	1234.4334	1234.42363	1355.5099	7.2	H5N2	Y	1355 (Int); 1193 (-H); 1014 (-N2AB); 869 (-3H); 707 (-4H); 545 (2N2AB); 528 (2HN); 487 (3H, Hyb/HM); 366 (HN); 342 (N2AB); 325 (2H)	
	A	1786.683	1665.6239	1665.60643	1786.7004	9.8	H3N5F1	Y	1786 (Int); 1640 (-F); 1583 (-N); 1437 (-F -N); 1380 (-2N); 1234 (-F -2N); 1218 (-2H); 1177 (-3N, CF); 1056 (-2N -2H , Bis + CF); 1031 (-3N -F); 1015 (-3N -H); 910 (H3N2AB, Bis); 853 (-3N -2H); 707 (-3N -2H -F); 691 (2NF2AB, CF); 488 (NF2AB, CF); 569 (2NH/Bis?); 545 (2N2AB); 366 (HN); 342 (N2AB); 325 (2H)	
8	B	1542.5827	1421.5179	1421.50613	1542.5944	7.6	H4N3F1	Y	1542 (Int); 1396 (-F); 1380 (-H); 1177 (-H -N, CF); 1031 (-HNF) 910 (H3N2AB, Bis); 707 (-3HNF); 691 (2NF2AB, CF); 488 (NF2AB, CF); 569 (2NH/Bis?); 545 (2N2AB); 528 (2HN); 366 (HN); 342 (N2AB); 325 (2H)	
	C	1583.6048	1462.5445	1462.52823	1583.6210	10.2	H3N4F1	N		
9		1786.6936	1665.6239	1665.61703	1786.7004	3.8	H3N5F1	N		
10		1825.6286	1704.5541	1704.55203	1825.6306	1.1	H4N4F1Su1	N		
	A	1745.6601	1624.5973	1624.58353	1745.6738	7.9	H4N4F1	Y	1745 (Int); 1599 (-F); 1583 (-H); 1437 (-H -F); 1380 (-H -N); 1234 (-H -N -F); 1218 (-2H -N); 1177 (-2NH, CF); 1072 (-2H -N -F); 910 (-3H -N -F, Bis); 691 (2NF2AB, CF); 488 (NF2AB, CF); 569 (2NH/Bis?); 545 (2N2AB); 528 (2HN); 366 (HN); 342 (N2AB); 325 (2H)	
11	B	1501.559	1380.4913	1380.48243	1501.5678	5.9	H5N2F1	Y	1501 (Int); 1355 (-F); 1339 (-H); 1117 (-2H); 1193 (-H -F); 1031 (-2H - F); 1014 (-2N2AB); 707 (2NH); 488 (NF2AB, CF); 545 (2N2AB); 528 (2HN); 366 (HN); 342 (N2AB); 325 (2H)	
	C	1558.5847	1437.5128	1437.50813	1558.5893	3.0	H5N3	Y	1558 (Int); 1396 (-H); 1234 (-2H); 1217 (-N2AB); 1072 (-3H); 1031 (-2HN); 1014 (-2N2AB); 852 (-H, -2N2AB); 910 (H3N2AB, Bis); 707 (-4HN); 569 (2NH/Bis?); 545	

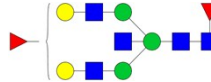
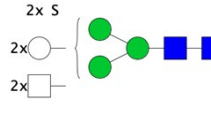
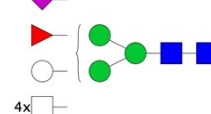
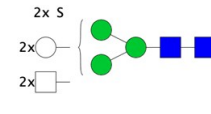
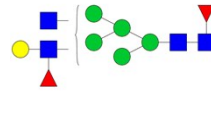
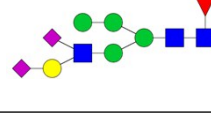
								(2N2AB); 528 (2HN); 366 (HN); 342 (N2AB)	
	D	1802.6876	1681.6188	1681.61103	1802.6953	4.3	H4N5	N	
12	A	1558.5801	1437.5128	1437.50353	1558.5893	5.9	H5N3	Y	1558 (Int); 1396 (-H); 1234 (-2H); 1217 (-N2AB); 1072 (-3H); 1031 (-2HN); 1014 (-2N2AB); 852 (-H, -2N2AB); 910 (H3N2AB, Bis); 707 (-4HN); 569 (2NH/Bis?); 545 (2N2AB); 528 (2HN); 366 (HN); 342 (N2AB); 325 (2H)
	B	1745.6623	1624.5973	1624.58573	1745.6738	6.6	H4N4F1	N	
	C	1825.6271	1704.5541	1704.55053	1825.6306	1.9	H4N4F1Su1	N	
13	A	1517.5512	1396.4862	1396.47463	1517.5627	7.6	H6N2	Y	1517 (Int); 1355 (-H); 1176 (-N2AB); 1193 (-2H); 1031 (-3H); 869 (-4H); 545 (2N2AB); 811 (5H, Hyb/HM); 545 (2N2AB); 528 (2HN); 487 (3H, Hyb/HM); 366 (HN); 342 (N2AB); 325 (2H)
	B	1745.6639	1624.5973	1624.58733	1745.6738	5.7	H4N4F1	N	
	C	1761.6573	1640.5922	1640.58073	1761.6687	6.5	H5N4	Y	1761 (Int); 1599 (-H); 1558 (-N); 1437 (-2H); 1420 (-N2AB); 1396 (-H-N); 1217 (-2N2AB); 1072 (-3H-N); 707 (-4H-2N); 569 (2NH/Bis?); 545 (2N2AB); 528 (2HN); 487 (3H, Hyb/HM); 342 (N2AB); 366 (NH); 325 (2H)
14	A	1517.551	1396.4862	1396.47443	1517.5627	7.7	H6N2	Y	1517 (Int); 1355 (-H); 1176 (-N2AB); 1193 (-2H); 1031 (-3H); 869 (-4H); 545 (2N2AB); 811 (5H, Hyb/HM); 545 (2N2AB); 528 (2HN); 487 (3H, Hyb/HM); 366 (HN); 342 (N2AB); 325 (2H)
	B	1597.4912	1476.4002	1476.41463	1597.4767	9.1	H3N4Su2	Y	1597 (Int); 1152 (-NSuH); 366 (HN)

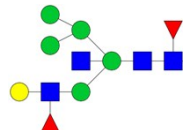
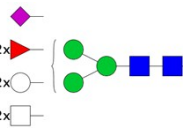
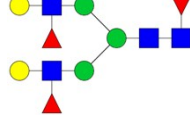
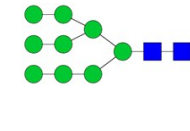
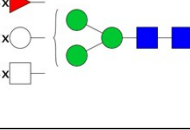
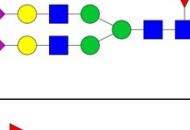
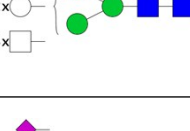
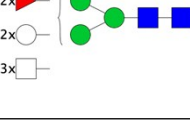
15	A	1761.6548	1640.5922	1640.57823	1761.6687	7.9	H5N4	Y	1761 (Int); 1599 (-H); 1558 (-N); 1437 (-2H); 1420 (-N2AB); 1396 (-H -N); 1275 (-3H); 1217 (-2N2AB); 1072 (-3H -N); 910 (H3N2AB, Bis); 707 (-4H -2N); 569 (2NH/Bis?); 545 (2N2AB); 528 (2HN); 487 (3H, Hyb/HM); 342 (N2AB); 366 (NH); 325 (2H)		
	B	1517.5514	1396.4862	1396.47483	1517.5627	7.5	H6N2	N			
16	A	1833.677	1712.6133	1712.6004	1833.6898	7.0	H4N3F1S1	Y	1833 (Int); 1687 (-F); 1671 (-H); 1542 (-S); 1525 (-FS); 1380 (-SH); 1346 (-NF2AB); 1234 (-SHF); 1177 (-SHN, CF); 1031 (-SHNF); 657 (SHN); 488 (NF2AB, CF); 454 (SH); 366 (HN); 342 (N2AB); 325 (2H)		
	B	1948.7375	1827.6767	1827.6609	1948.7532	8.1	H4N5F1	N			
	C	1761.6727	1640.5922	1640.5961	1761.6687	2.3	H5N4	N			
	D	1745.675	1624.5973	1624.5984	1745.6738	0.7	H4N4F1	N			
17	A	1891.7153	1770.6552	1770.6387	1891.7317	8.7	H4N4F2	Y	1891 (Int); 1745 (-F); 1729 (-H); 1599 (-2F); 1583 (-H -F); 1437 (-H -2F); 1404 (-N2AB); 1380 (-H -N -F); 1234 (-H -N -2F); 1201 (-2N2AB); 1177 (-2NHF, CF); 1072 (-2H -N -N -2F); 1056 (-HNF, Bis + CF); 910 (H3N2AB, Bis); 707 (-4H -N -2F); 691 (2NF2AB, CF); 569 (2NH/Bis?); 545 (2N2AB); 528 (2HN); 512 (HNF, AF); 488 (NF2AB, CF); 342 (N2AB); 366 (NH); 325 (2H)		
	B	1907.7127	1786.6501	1786.6361	1907.7266	7.3	H5N4F1	N			
	C	2003.617	1882.5590	1882.5404	2003.6355	9.2	H3N6Su2	N			

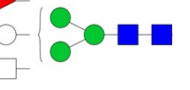
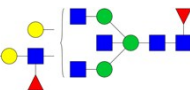
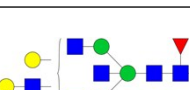
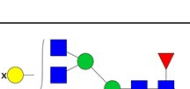
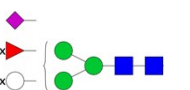
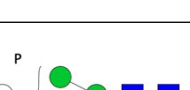
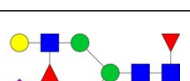
	A	1907.7116	1786.6501	1786.6350	1907.7266	7.9	H5N4F1	Y	1907 (Int); 1761 (-F); 1745 (-H); 1704 (-N); 1599 (-H -F); 1583 (-2H); 1501 (-2N); 1437 (-2H -F); 1420 (-N2AB); 1339 (-2NH); 1234 (-2H -F -N); 1217 (-2N2AB); 1177 (-2H2N, CF); 1031 (-2N2HF); 1015 (-2N3H); 910 (3NH2AB, Bis); 852 (-H -2N -N2AB -F); 691 (2NF2AB, CF); 569 (2NH/Bis?); 545 (2N2AB); 528 (2HN); 488 (NF2AB, CF); 342 (N2AB); 366 (NH); 325 (2H)	
18	B	2003.6247	1882.5590	1882.5481	2003.6355	5.4	H3N6Su2	N		
	C	1891.7162	1770.6552	1770.6396	1891.7317	8.2	H4N4F2	N		
	A	2094.8139	1973.7346	1973.73733	2094.8111	1.3	H4N5F2	Y	2094 (Int); 1948 (-F); 1932 (-H); 1891 (-N); 1802 (-2F); 1786 (-H -F); 1607 (-N2AB); 1583 (-H -F -N); 1437 (-H -2F -N); 1404 (-2N2AB); 1380 (-H -F -2N); 1218 (-2H -F -2N); 1177 (-3NHF, CF); 1056 (3H -F -2N , Bis + CF); 910 (H3N2AB, Bis); 853 (-3H -2F -3N); 691 (2NF2AB, CF); 569 (2NH/Bis?); 545 (2N2AB); 528 (2HN); 512 (HNF, AF); 488 (NF2AB, CF); 366 (NH); 342 (N2AB)	
19	B	1891.7159	1770.6552	1770.63933	1891.7317	8.4	H4N4F2	Y	1891 (Int); 1745 (-F); 1729 (-H); 1599 (-2F); 1583 (-H -F); 1437 (-H -2F); 1404 (-N2AB); 1380 (-H -N - F); 1234 (-H - N - 2F); 1218 (-2HNF); 1201 (-2N2AB); 1177 (-2NHF, CF); 1072 (-2H -N -2F); 707 (-4H -N - 2F); 569 (2NH/Bis?); 545 (2N2AB); 528 (2HN); 512 (HNF, AF); 488 (NF2AB, CF); 342 (N2AB)	
	A	1679.6038	1558.5390	1558.52723	1679.6155	7.0	H7N2	Y	1679 (Int); 1517 (-H); 1355 (-2H); 1338 (-N2AB); 1193 (-3H); 1176 (-H, -N2AB); 811 (5H, Hyb/HM); 649 (4H, Hyb/HM); 545 (2N2AB); 528 (2HN); 487 (3H, Hyb/HM); 366 (NH); 342 (N2AB); 325 (2H)	
20	B	2094.8131	1973.7346	1973.73653	2094.8111	0.9	H4N5F2	Y	2094 (Int); 1948 (-F); 1932 (-H); 1891(-N); 1802 (-2F); 1729 (-HN); 1607 (-N2AB); 1583 (-H -F -N); 1437 (-H -2F -N); 1404 (-2N2AB); 1380 (-H -F -2N); 1218 (-2H -F -2N); 1056 (-3H -F -2N , Bis + CF); 910 (H3N2AB, Bis); 691 (2NF2AB, CF); 569 (2NH/Bis?); 545 (2N2AB); 528 (2HN); 512 (HNF, AF); 488 (NF2AB, CF); 366 (NH); 342 (N2AB); 325 (2H)	

	C	1850.6895	1729.6286	1729.61293	1850.7051	8.4	H5N3F2	Y	1850 (Int); 1177 (3H2NF2AB, CF); 545 (2N2AB); 528 (2HN); 512 (HNF, AF); 488 (NF2AB, CF); 342 (N2AB)	
21	A	2053.7686	1932.7080	1932.6920	2053.7845	7.8	H5N4F2	Y	2053 (Int); 1907 (-F); 1891 (-H); 1762 (-2F); 1745 (-HF); 1729 (-2H); 1688 (-HN); 1566 (-N2AB); 1526 (-2HN); 1380 (-2H -N -F); 1234 (-2H -N -2F); 1363 (-2N2AB); 1177 (-2H -2N -F, CF); 853 (-3H -2N -F); 836 (3HNF); 691 (2NF2AB, CF); 674 (2HNF); 569 (2NH/Bis?); 545 (2N2AB); 528 (2HN); 512 (HNF, AF); 488 (NF2AB, CF); 366 (NH); 342 (N2AB)	
	B	1995.7349	1874.6661	1874.65833	1995.7426	3.9	H5N3F1S1	Y	1995 (Int); 1849 (-F); 1704 (-S); 1558 (-SF); 1542 (-SH); 1339 (-SHN); 1177 (-2HNS, CF); 657 (SHN); 545 (2N2AB); 528 (2HN); 488 (NF2AB, CF); 454 (HS); 366 (NH); 342 (N2AB); 325 (2H)	
	C	2094.8087	1973.7346	1973.73213	2094.8111	1.2	H4N5F2	N		
	D	2149.6845	2028.6169	2028.60793	2149.6934	4.2	H3N6F1Su2	N		
	E	2239.8511	2118.7721	2118.77453	2239.8486	1.1	H4N5F1S1	N		
22	A	1597.5227	1476.4525	1476.44613	1597.5290	4.0	H6N2P1	Y	1597 (Int); 1435 (-H (P)); 1273 (-2H (P)); 1256 (-N2AB (P)); 1111 (-3H (P)); 567 (3H (P)); 545 (2N2AB); 528 (2HN); 405 (2H (P)); 366 (NH); 342 (N2AB); 325 (2H)	
	B	1995.7349	1874.6661	1874.65832	1995.7426	3.9	H5N3F1S1	Y	1995 (Int); 1849 (-F); 1704 (-S); 1558 (-SF); 1542 (-SH); 1339 (-SHN); 1177 (-2HNS, CF); 657 (SHN); 545 (2N2AB); 528 (2HN); 488 (NF2AB, CF); 454 (HS); 366 (NH); 342 (N2AB); 325 (2H)	

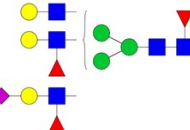
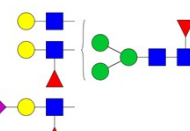
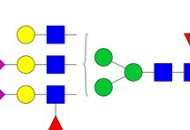
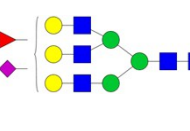
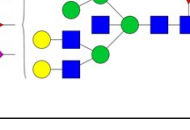
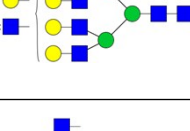
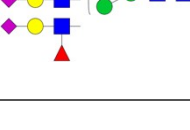
	C	2239.8434	2118.7721	2118.76683	2239.8486	2.3	H4N5F1S1	Y	2239 (Int); 1948 (-S); 1786 (-SH); 1752 (-NF2AB); 1583 (-SHN); 1549 (-N2F2AB); 1380 (-SH2N); 1234 (-SHF2N); 910 (H3N2AB, Bis); 657 (SHN); 569 (2NH/Bis?); 545 (2N2AB); 528 (2HN); 488 (NF2AB, CF); 454 (SH); 366 (NH); 342 (N2AB)	
	D	2053.7739	1932.7080	1932.69733	2053.7845	5.2	H5N4F2	N		
	E	2198.8124	2077.7455	2077.73583	2198.8220	4.4	H5N4F1S1	N		
	F	1800.5961	1679.5224	1679.51953	1800.5989	1.6	H6N3Su1	N		
23		2069.7724	1948.7029	1948.69583	2069.7794	3.4	H6N4F1	Y	2069 (Int); 1379 (-2N2AB); 1217 (-H -2N2AB); 1014 (-H -N -2N2AB); 852 (-2H -N -2N2AB); 691 (2NF2AB, CF); 545 (2N2AB); 528 (2HN); 488 (NF2AB, CF); 366 (NH)	
	A	2297.8949	2176.8140	2176.81833	2297.8905	1.9	H4N6F2	Y	1149.4514 (Int, 2+); 1056 (-3H -F -2N, Bis + CF); 910 (H3N2AB, Bis); 691 (2NF2AB, CF); 569 (2NH/Bis?); 545 (2N2AB); 528 (2HN); 512 (HNF, AF); 488 (NF2AB, CF); 366 (NH)	
24	B	2442.9253	2321.8515	2321.84873	2442.9280	1.1	H4N6F1S1	N		
25	A	1841.6559	1720.5918	1720.57933	1841.6683	6.7	H8N2	Y	1841 (Int); 1679 (-H); 1517 (-2H); 1500 (-N2AB); 811 (5H, Hyb/HM); 649 (4H, Hyb/HM); 545 (2N2AB); 528 (2HN); 487 (3H, Hyb/HM); 366 (NH); 342 (N2AB); 325 (2H)	

	B	2256.8664	2135.7874	2135.78983	2256.8639	1.1	H5N5F2	Y	2256 (Int); 2110 (-F); 1769 (-NF2AB); 1745 (-HNF); 1583 (-2HNF); 1566 (-2NF2AB); 1380 (-2H2N2F); 691 (2NF2AB, CF); 569 (2NH/Bis?); 545 (2N2AB); 528 (2HN); 512 (HNF, AF); 488 (NF2AB, CF); 366 (NH); 342 (N2AB)	
	C	2198.8192	2077.7455	2077.74263	2198.8220	1.3	H5N4F1S1	N		
	D	1921.5991	1800.5058	1800.52253	1921.5823	8.7	H5N4Su2	N		
	E	2442.9277	2321.8515	2321.85113	2442.9280	0.1	H4N6F1S1	N		
26	A	1841.6555	1720.5918	1720.57893	1841.6683	7.0	H8N2	Y	1841 (Int); 1679 (-H); 1517 (-2H); 1500 (-N2AB); 1355 (-3H); 1193 (-4H); 1031 (-5H); 973 (6H, Hyb/HM); 869 (-6H); 811 (5H, Hyb/HM); 707 (-7H); 649 (4H, Hyb/HM); 545 (2N2AB); 528 (2HN); 487 (3H, Hyb/HM), 366 (NH); 342 (N2AB); 325 (2H)	
	B	1921.5991	1800.5058	1800.52253	1921.5823	8.7	H5N4Su2	N		
27	A	2215.83	2094.7608	2094.7534	2215.8373	3.3	H6N4F2	Y	2215 (Int); 2053 (-H); 1704 (-HNF); 1542 (-2HNF); 691 (2NF2AB, CF); 569 (2NH/Bis?); 545 (2N2AB); 528 (2HN); 512 (HNF, AF); 488 (NF2AB, CF); 366 (NH); 342 (N2AB)	
	B	2286.8465	2165.7615	2165.7699	2286.8381	3.7	H5N3F1S2	Y	2286.8097 (Int); 1177 (3H2NF2AB, CF); 948 (Di-Sialyl Lewis C); 657 (SHN); 545 (2N2AB); 528 (2HN); 495 (SN); 488 (NF2AB, CF)	

	A	2215.8305	2094.7608	2094.7539	2215.8373	3.1	H6N4F2	Y	2215 (Int); 2053 (-H); 1704 (-HNF); 1542 (-2HNF); 910 (3NH2AB, Bis); 691 (2NF2AB, CF); 569 (2NH/Bis?); 545 (2N2AB); 528 (2HN); 512 (HNF, AF); 488 (NF2AB, CF); 366 (NH); 342 (N2AB)	
28	B	2344.872	2223.8034	2223.7954	2344.8799	3.4	H5N4F2S1	N		
	C	2199.8453	2078.7659	2078.7687	2199.8424	1.3	H5N4F3	Y	2199 (Int); 2053 (-F); 1712 (-N2AB); 1688 (-H -N -F); 1526 (-2H -N -F); 1177 (-2H -2N -2F, CF); 674 (2HNF); 545 (2N2AB); 528 (2HN); 512 (HNF, AF); 488 (NF2AB, CF); 366 (HN); 342 (N2AB)	
	A	2003.7058	1882.6446	1882.6292	2003.7211	7.6	H9N2	Y	2003 (Int); 1841 (-H); 1679 (-2H); 1662 (-N2AB); 1517 (-3H); 1355 (-4H); 1193 (-5H); 1031 (-5H); 973 (6H, Hyb/HM); 869 (-6H); 811 (5H, Hyb/HM); 649 (4H, Hyb/HM); 487 (3H, Hyb/HM); 545 (2N2AB); 528 (2HN); 366 (HN); 342 (N2AB); 325 (2H).	
29	B	2402.9225	2281.8453	2281.8459	2402.9218	0.3	H5N5F3	N		
	A	2489.9197	2368.8409	2368.8431	2489.9174	0.9	H5N4F1S2	Y	1245.4656 (Int, 2+); 1177 (-2S2H2N, CF); 657 (SHN); 569 (2NH/Bis?); 545 (2N2AB); 528 (2HN); 488 (NF2AB, CF); 454 (SH); 366 (NH)	
	B	2402.9407	2281.8453	2281.8641	2402.9218	7.9	H5N5F3	N		
30	C	2547.9635	2426.8828	2426.88693	2547.9593	1.6	H5N5F2S1	N		

	D	2003.7022	1882.6446	1882.6256	2003.7211	9.4	H9N2	N		
	E	2361.89	2240.8187	2240.8134	2361.8952	2.2	H6N4F3	N		
31	A	2751.0454	2629.9622	2629.96883	2751.0387	2.4	H5N6F2S1	Y	1376.0269 (Int, 2+); 1056 (-S -4H -F -4N , Bis + CF); 803 (SHNF); 691 (2NF2AB, CF); 657 (SHN); 569 (2NH/Bis?); 545 (2N2AB); 528 (2HN); 512 (HNF, AF); 488 (NF2AB, CF); 454 (SH); 366 (NH)	
	B	2402.9152	2281.8453	2281.8386	2402.9218	2.8	H5N5F3	N		
32	A	2751.0597	2629.9622	2629.9831	2751.0387	7.6	H5N6F2S1	Y	1376.0226 (Int, 2+); 1056 (-S -4H -F -4N , Bis + CF); 803 (SHNF); 691 (2NF2AB, CF); 657 (SHN); 569 (2NH/Bis?); 545 (2N2AB); 528 (2HN); 512 (HNF, AF); 488 (NF2AB, CF); 454 (SH); 366 (NH)	
	B	2606.0072	2484.9247	2484.9306	2606.0012	2.3	H5N6F3	Y	1303.5068 (Int, 2+); 691 (2NF2AB, CF); 569 (2NH/Bis?); 545 (2N2AB); 528 (2HN); 512 (HNF, AF); 488 (NF2AB, CF); 366 (NH)	
33	C	2344.8836	2223.8034	2223.8070	2344.8799	1.6	H5N4F2S1	N		
		2165.7558	2044.6641	2044.6792	2165.7406	7.0	H7N4P1	N		
34		2635.9883	2514.8988	2514.9117	2635.9753	4.9	H5N4F2S2	Y	1318.4985 (Int, 2+); 948 (Di-Sialyl Lewis C); 657 (SHN); 545 (2N2AB); 528 (2HN); 512 (HNF, AF); 495 (SN); 488	

								(NF2AB, CF); 454 (SH); 366 (NH)	
35	A	2781.0361	2659.9363	2659.9595	2781.0128	8.4	H5N4F1S3	Y	1391.0172 (Int, 2+); 1177 (-3S-2H-2N, CF); 948 (Di-Sialyl Lewis C); 657 (SHN); 545 (2N2AB); 528 (2HN); 495 (SN); 488 (NF2AB, CF); 454 (SH); 366 (NH)
	B	2954.1348	2833.0416	2833.0582	2954.1181	5.6	H5N7F2S1	Y	1477.5587 (Int, 2+); 691 (2NF2AB, CF); 657 (SHN); 569 (2NH/Bis?); 545 (2N2AB); 512 (HNF, AF); 488 (NF2AB, CF); 366 (NH)
36		3042.1615	2921.0576	2921.08493	3042.1341	9.0	H5N6F2S2	Y	1521.5854 (Int, 2+); 948 (Di-Sialyl Lewis C); 691 (2NF2AB, CF); 657 (SHN); 545 (2N2AB); 528 (2HN); 512 (HNF, AF); 495 (SN); 488 (NF2AB, CF); 454 (SH); 366 (NH)
37		3099.1646	2978.0791	2978.08803	3099.1556	2.9	H5N7F1S2	Y	1550.0871 (Int, 2+); 691 (2NF2AB, CF); 657 (SHN); 454 (SH); 366 (HN)
38		2984.0954	2863.0157	2863.01883	2984.0922	1.1	H5N5F1S3	N	
39		-	-	-	-	-	-	-	-
40	A	2711.0469	2589.9560	2589.97033	2711.0325	5.3	H6N5F4	Y	1356.0256 (Int, 2+); 691 (2NF2AB, CF); 545 (2N2AB); 528 (2HN); 512 (HNF, AF); 488 (NF2AB, CF); 366 (NH)
	B	3059.151	2938.0729	2938.07443	3059.1494	0.5	H6N6F3S1	Y	1530.0842 (Int, 2+); 803 (SHNF); 691 (2NF2AB, CF); 657 (SHN); 569 (2NH/Bis?); 545 (2N2AB); 528 (2HN); 512 (HNF, AF); 488 (NF2AB, CF); 454 (SH); 366 (NH)

	C	2856.0722	2734.9935	2734.99563	2856.0700	0.8	H6N5F3S1	Y	1428.5416 (Int, 2+); 803 (SHNF); 657 (SHN); 528 (2HN); 512 (HNF, AF); 488 (NF2AB, CF); 366 (NH)	
41		2856.0767	2734.9935	2735.00013	2856.0700	2.3	H6N5F3S1	Y	1428.5438 (Int, 2+); 803 (SHNF); 691 (2NF2AB, CF); 657 (SHN); 545 (2N2AB); 528 (2HN); 512 (HNF, AF); 488 (NF2AB, CF); 454 (SH); 366 (NH)	
	A	3001.1207	2880.0310	2880.04413	3001.1075	4.4	H6N5F2S2	Y	1501.0598 (Int, 2+); 803 (SHNF); 691 (2NF2AB, CF); 657 (SHN); 545 (2N2AB); 528 (2HN); 512 (HNF, AF); 488 (NF2AB, CF); 454 (SH); 366 (NH)	
	B	2856.0731	2734.9935	2734.99653	2856.0700	1.1	H6N5F3S1	N		
42	C	2952.0876	2830.9547	2831.01103	2952.0645	19.1	H7N5F2S1P1	Y	1476.5499 (Int, 2+); 910 (H3N2AB, Bis); 657 (SHN); 528 (2HN); 512 (HNF, AF); 488 (NF2AB, CF); 366 (NH)	
	D	3060.1448	2939.0682	2939.06823	3060.1447	0.0	H8N8	N		
	E	3204.1862	3083.1104	3083.10963	3204.1869	0.2	H6N6F2S2	Y	1602.5936 (Int, 2+); 803 (SHNF); 657 (SHN); 545 (2N2AB); 512 (HNF, AF); 488 (NF2AB, CF); 366 (NH)	

	A	2856.073	2734.9935	2734.99643	2856.0700	1.0	H6N5F3S1	Y	1428.5212 (Int, 2+); 803 (SHNF); 657 (SHN); 545 (2N2AB); 528 (2HN); 512 (HNF, AF); 488 (NF2AB, CF); 366 (NH)	
43	B	3146.1361	3025.0685	3025.05953	3146.1450	2.8	H6N5F1S3	Y	1573.5708 (Int, 2+); 657 (SHN); 528 (2HN); 512 (HNF, AF); 454 (SH); 366 (NH)	
	C	3059.1513	2938.0729	2938.07473	3059.1494	0.6	H6N6F3S1	Y	1530.0888 (Int, 2+); 803 (SHNF); 691 (2NF2AB, CF); 657 (SHN); 545 (2N2AB); 512 (HNF, AF); 488 (NF2AB, CF); 366 (NH)	
	D	3097.1227	2975.9922	2976.04613	3097.1020	17.4	H7N5F1S2P1	N		
	A	3001.1261	2880.0310	2880.04953	3001.1075	6.2	H6N5F2S2	Y	1501.0799 (Int, 2+); 803 (SHNF); 657 (SHN); 528 (2HN); 512 (HNF, AF); 488 (NF2AB, CF); 366 (NH)	
44	B	3262.2224	3141.1523	3141.14583	3262.2288	2.0	H6N7F3S1	Y	1631.6172 (Int, 2+); 691 (2NF2AB, CF); 657 (SHN); 512 (HNF, AF); 488 (NF2AB, CF); 366 (NH)	
	C	3204.1857	3083.1104	3083.10913	3204.1869	0.4	H6N6F2S2	Y	1602.5952 (Int, 2+); 803 (SHNF); 657 (SHN); 528 (2HN); 512 (HNF, AF); 488 (NF2AB, CF); 454 (SH); 366 (NH)	
	D	3147.1426	3026.0889	3026.06603	3147.1654	7.3	H6N5F3S2	Y	1574.0702 (Int, 2+); 948 (Di-Sialyl Lewis C); 657 (SHN); 528 (2HN); 512 (HNF, AF); 495 (SN); 488 (NF2AB, CF); 366 (NH)	

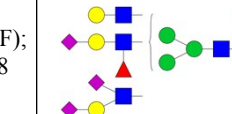
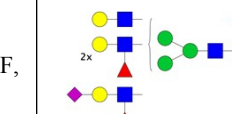
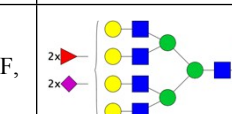
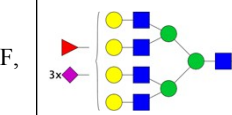
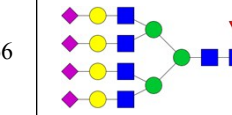
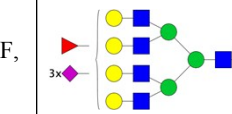
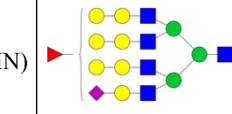
45		-	-	-	-	-	-	-	-	-	-
46		3292.1921	3171.1264	3171.11553	3292.2029	3.3	H6N5F2S3	Y	1646.6024 (Int, 2+); 948 (Di-Sialyl Lewis C); 803 (SHNF); 657 (SHN); 528 (2HN); 512 (HNF, AF); 495 (SN); 488 (NF2AB, CF); 454 (SH); 366 (NH)		
47		3367.2671	3246.1836	3246.19053	3367.2601	2.1	H7N6F4S1	Y	1684.1317 (Int, 2+); 803 (SHNF); 657 (SHN); 512 (HNF, AF); 488 (NF2AB, CF); 366 (NH)		
	A	3512.291	3391.2211	3391.21443	3512.2976	1.9	H7N6F3S2	Y	1756.6328 (Int, 2+); 803 (SHNF); 657 (SHN); 512 (HNF, AF); 488 (NF2AB, CF); 454 (SH); 366 (NH)		
48	B	3657.3498	3536.2586	3536.27323	3657.3351	4.0	H7N6F2S3	Y	1829.1770 (Int, 2+); 803 (SHNF); 657 (SHN); 512 (HNF, AF); 488 (NF2AB, CF); 454 (SH); 366 (NH)		
	C	3802.3761	3681.2961	3681.29953	3802.3726	0.9	H7N6F1S4	Y	1901.6887 (Int, 2+); 657 (SHN); 488 (NF2AB, CF); 366 (NH)		
49		3657.3559	3536.2586	3536.27933	3657.3351	5.7	H7N6F2S3	Y	1829.1786 (Int, 2+); 803 (SHNF); 657 (SHN); 512 (HNF, AF); 488 (NF2AB, CF); 366 (NH)		
50		3415.2528	3294.1683	3294.17623	3415.2448	2.3	H10N6F1S1	Y	1708.1232 (Int, 2+); 657 (SHN); 512 (HNF, AF); 366 (HN)		

Table ST-2. Mass spectrometry analysis of samples prepared by LSD and HSD (10 mg). Structures within one chromatographic section (i.e., A, B, C ...) are listed in order of decreasing abundance. CS = Chromatographic Section; GS = Glycan Structure (Green = good confidence; Yellow = reasonable; Red = low confidence); MMM = Measured Monoisotopic Mass, $[M+2AB+H]^+$ (Red= LSD only; White = both methods); MUM = Measured Unlabeled Monoisotopic Glycan Mass; TUM = Theoretical Unlabeled Monoisotopic Glycan Mass; TLM = Theoretical Labeled Monoisotopic Mass

$[M+2AB+H]^+$; RMA = Relative Mass Accuracy ($(|MMMM-TLM|/TLM) * 10^6$); MC = Monosaccharide Composition; MS² = Fragmentation data (Y = Informative or partially informative fragments; N = No fragments); DFI = Diagnostic Fragments Identified (Red = fragmentation spectra found only in the LSD sample; Blue = fragmentation spectra found only in the HSD sample; White = fragmentation spectra found in both LSD and HSD samples; H = Hexose, N = N-Acetylhexosamine, F = Deoxyhexose (Fucose), S = N-Acetylneuraminic Acid (Sialic acid), Su = Sulphate, P = Phosphate; Int = Intact, precursor ion chosen for fragmentation and relative charge state, if not singly charged. In the case of singly charged ions, the intact signal equals the MMM value. All the listed fragments are mono-protonated, singly charged fragments); CF = Core Fucose, AF = Antennary Fucose, Bis = Bisecting, Hyb/HM = Hybrid/High Mannose, 2AB = 2-Aminobenzamide); PGS = Proposed Glycan Structure (N-glycan structures are depicted without 2-AB).

Table ST-3. Examples of glycoproteins, glycopeptides and glycosylation sites identified by downstream proteomics applications using the LSD lysate.

IgP	UPI	pC	SC (%)	NDS	UP?	MW (kDa)	IPe	IPe m/z	IPe Ch.	IPe RT (min)	IPe ME (ppm)	F
Neural cell adhesion molecule 1	F1LNY3	2	3	N444	N	92.721	ALASEWKPEIR DGQLLPSS[NYSNIK]	768.8806 650.3564	2+ 2+	36.30 37.20	1.5 6.0	1
Contactin-1	Q63198	3	4.5	N494	Y	113,495	A[NSTGTLVITNPTR TDGAAPNVAPSVDVGGGGTNR VQVTSQEYSAR]	723.3833 935.4379 634.3174	2+ 2+ 2+	32.40 25.30 23.50	4.1 6.4 0.8	2
Myelin-associated glycoprotein	PO7722	3	8.1	N99	Y	64.291*	[NCTLLLSTLSPELGGK NLYGTQSLELPFQGAHR SNPEPSVAFELPSR]	852.4478 965.9921 765.3833	2+ 2+ 2+	50.67 45.76 40.49	3.0 0.7 0.9	3
Excitatory amino acid transporter 2	P31596	2	4.4	N205	Y	62.106**	SELDTIDSQHR VLVAPPSEEATTK	650.810 728.8801	2+ 2+	26.01 29.27	0.2 0.6	4, 5, 6
Dihydropyrimidinase-related protein 2	P47942	14	37.4	N356	N	62.28	DIGAIAQVHAENGDIIEEEQQR DNFTLIPEGTN[NGTEER FQMPDQGMTSADDFFQGTK GLYDGPVCEVSVPK GSPLVVVISQGK GTVVYGEPIASLGTDGSHYWSK ISVGSDADLVIWDPDSVK IVLEDGTLHVTEGSGR MDENQFVAVTSTNAAK MVIPGGIDVHTR QIGENLIVPGGVK SAAEAVIAQAR SITIANQTNCPLYVTK VFNLNYPYR	1189.090 897.4130 1091.956 810.9005 1084.636 1213.087 958.4860 841.9390 871.4067 655.8479 1323.763 1015.553 911.9720 908.4988	2+ 2+ 2+ 2+ 1+ 2+ 2+ 2+ 2+ 2+ 1+ 1+ 2+ 1+	40.11 39.64 39.15 38.34 34.72 45.45 50.39 36.42 31.66 33.09 39.82 27.41 38.06 38.06	1.2 6 2.8 1.3 3.6 1.6 1.4 3.5 4.0 3.2 0.1 1.5 2 1.2	7
BTB domain-containing 18	D3Z9A5	1	2.2	N201	N	79.27	SNLPNAD[N]SDTLLK	865.4463	2+	39.56	5.0	9
Sodium/potassium-transporting ATPase subunit beta-2	P13638	1	4.5	N238	Y	33.40	FHV[N]YTQPLVAVK	758.9115	2+	41.66	1.9	11
Thy-1 membrane glycoprotein	P01830	1	6.2	N93	Y	18.17	VLTLA[N]FTTK	1108.624	1+	45.30	1.2	17

Table ST-3. Examples of glycoproteins identified by downstream proteomics applications using the LSD lysate. Identified glycoproteins demonstrate the suitability of the LSD lysate for glycoproteomics analyses. IgP = identified glycoprotein; UPI = Uniprot KB identifier; pC = peptide count (unique deglycosylated peptides); SC = sequence coverage (unique deglycosylated peptides); NDS = experimentally highlighted Asn→Asp site position; UP? = was the N-glycosylation at given site reported in Uniprot KB before this analysis?; MW (kDa) = Uniprot KB sequence-based theoretical MW (N-glycosylation not considered); IPe = identified deglycosylated peptides (NDS site is highlighted in green); IPe m/z = identified deglycosylated peptides mass to charge ratio; IPe Ch. = identified deglycosylated peptides charge; IPe RT = identified deglycosylated peptides retention time; IPe ME = identified deglycosylated peptide mass error (ppm); F = SDS-PAGE fraction in which the glycoprotein has been identified; *protein homodimerization reported (Uniprot KB); **protein homotrimerization reported (Uniprot KB).

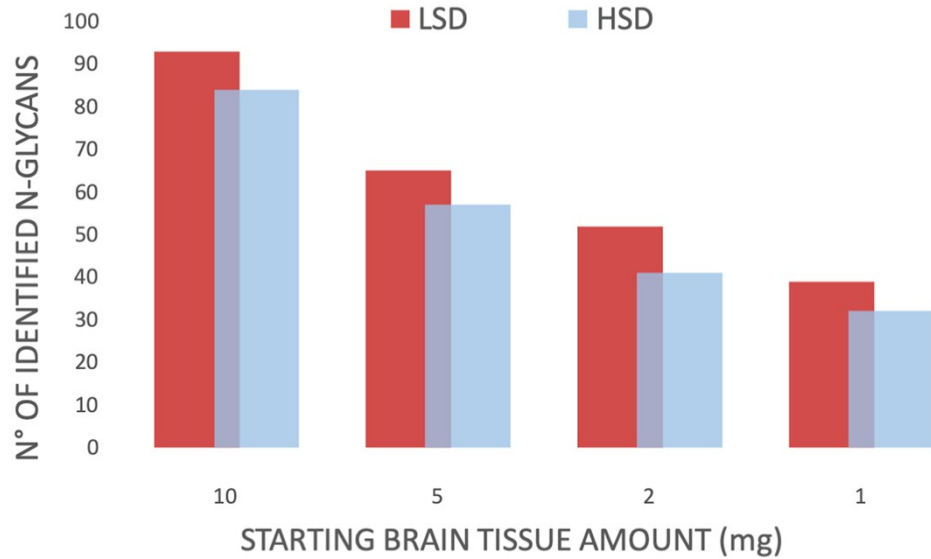
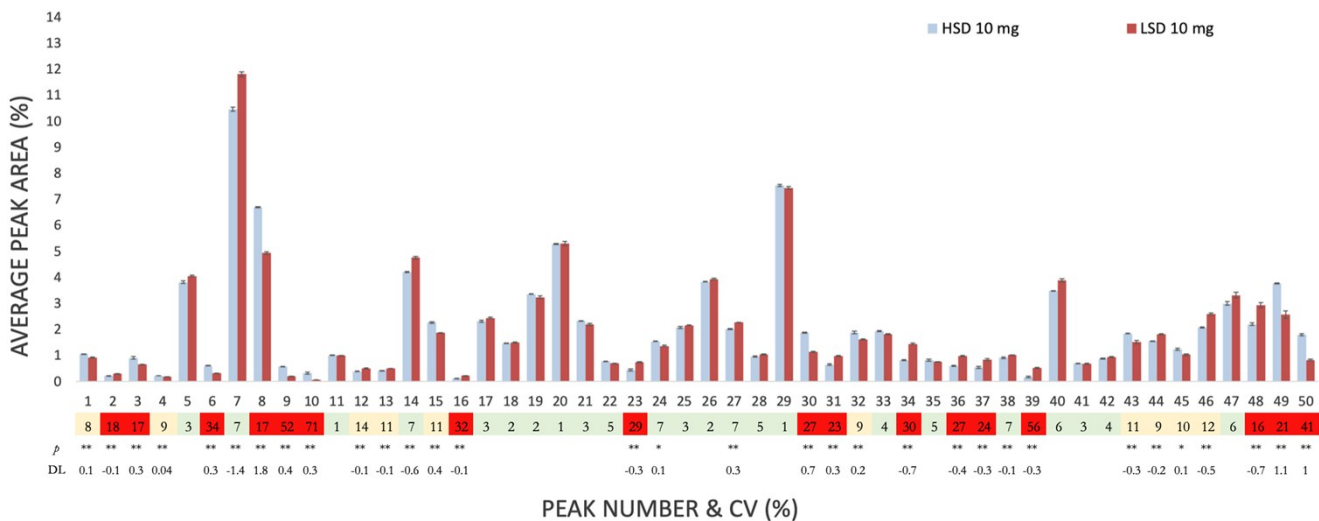
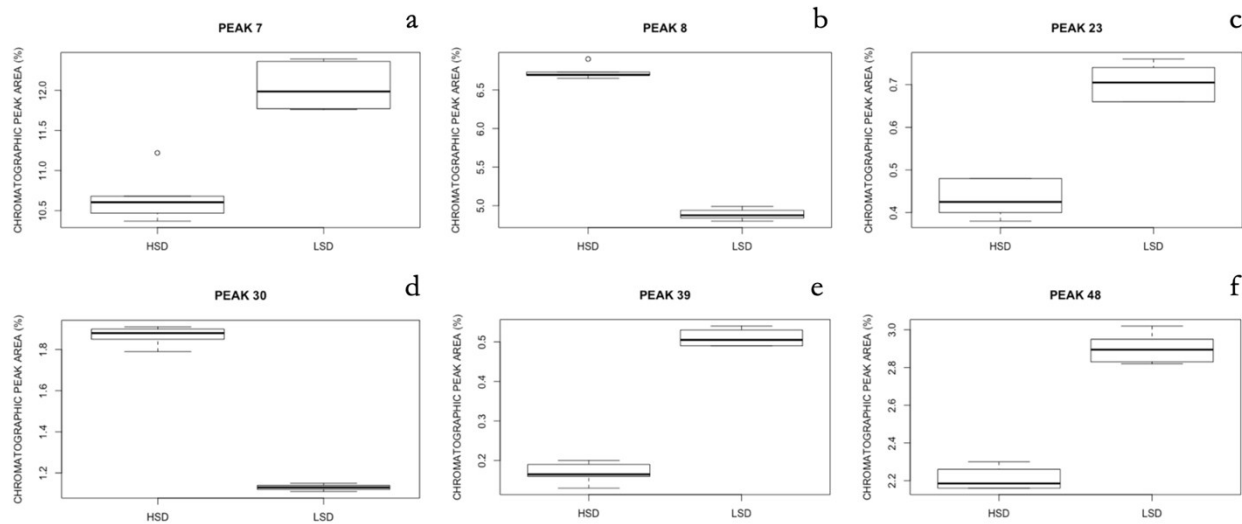


Figure S-14. LSD and HSD structural resolution on each starting brain tissue amount.

A



B



a: m[q] LSD = 11.98 [11.81, 12.28]; HSD = 10.61 [10.48, 10.68]; U = 0; p < 0.01; 0.95 CI [-1.83, -1.1]; DL = -1.40

b: m[q] LSD = 4.87 [4.85, 4.92]; HSD = 6.69 [6.69, 6.72]; U = 36; p < 0.01; 0.95 CI [1.74, 1.93]; DL = 1.82

c: m[q] LSD = 0.70 [0.67, 0.73]; HSD = 0.42 [0.40, 0.47]; U = 0; p < 0.01; 0.95 CI [-0.34, -0.21]; DL = -0.28

d: m[q] LSD = 1.13 [1.12, 1.14]; HSD = 1.9 [1.85, 1.87]; U = 36; p < 0.01; 0.95 CI [0.68, 0.78]; DL = 0.75

e: m[q] LSD = 0.5 [0.49, 0.52]; HSD = 0.16 [0.16, 0.17]; U = 0; p < 0.01; 0.95 CI [-0.37, -0.31]; DL = -0.34

f: m[q] LSD = 2.89 [2.83, 2.95]; HSD = 2.18 [2.16, 2.24]; U = 0; p < 0.01; 0.95 CI [-0.79, -0.58]; DL = -0.67

Figure S-15. Comparison of the profiles obtained by LSD^{μL} and HSD. **A.** Quantitative comparison of LSD^{μL} and HSD chromatograms (10 mg profiles, representing samples showing the richest N-glycomic profiles, are displayed as an example). Descriptive error bars show data spread within replicates ($n = 1$, triplicates) as \pm SD. CV for each peak is reported as a measure of precision of the value of the same peak area between the two methods (green = $CV \leq 7\%$; yellow = $7\% < CV \leq 15\%$; red = $CV > 15\%$). The statistical analysis (Wilcoxon-Mann-Whitney, $n = 2$, triplicates, HSD Vs LSD^{μL}, calculated using values of peak chromatographic areas deriving from both the 10 mg and 5 mg samples to improve the statistical outcome. The 10 and 5 mg samples from both methods show very similar aCVs (see Figure 1) and the same dominant N-glycan structure for each peak (data not shown). p-values (* $p < 0.05$, ** $p < 0.01$) and DL values for each peak comparison ($CVs > 7\%$) are displayed. **B.** Box-plots indicate dispersion and skewness of the data for six peaks present in A, and the related statistical analysis is summarized in the lower part of the image through the presentation of relevant parameters.

Increased abundance in HSD		Increased abundance in LSD	
Fraction	Proposed N-glycan type	Fraction	Proposed N-glycan type
1	Paucimannose	2	Paucimannose
3	Paucimannose	7	Oligomannose
4	Paucimannose	12	Hybrid
6	Complex	13	Oligomannose
8	Complex	14	Oligomannose
9	Complex	16	Complex sialylated
10	Complex	23	Hybrid
15	Oligomannose	27	Hybrid
24	Complex	31	Complex sialylated
30	Oligomannose	34	Complex sialylated
32	Complex sialylated	36	Complex sialylated
43	Complex sialylated	37	Complex sialylated
45	Not determined	38	Complex sialylated
49	Complex sialylated	39	Not determined
50	Not determined	44	Complex sialylated
		46	Complex sialylated
		48	Complex sialylated

Figure S-16. Chromatographic sections whose abundance is significantly different between methods by N-glycan type and the proposed N-glycan type of the dominant N-glycan structure present in each section.

Peak 22 – Structure 22F is uniquely identified by the LSD method

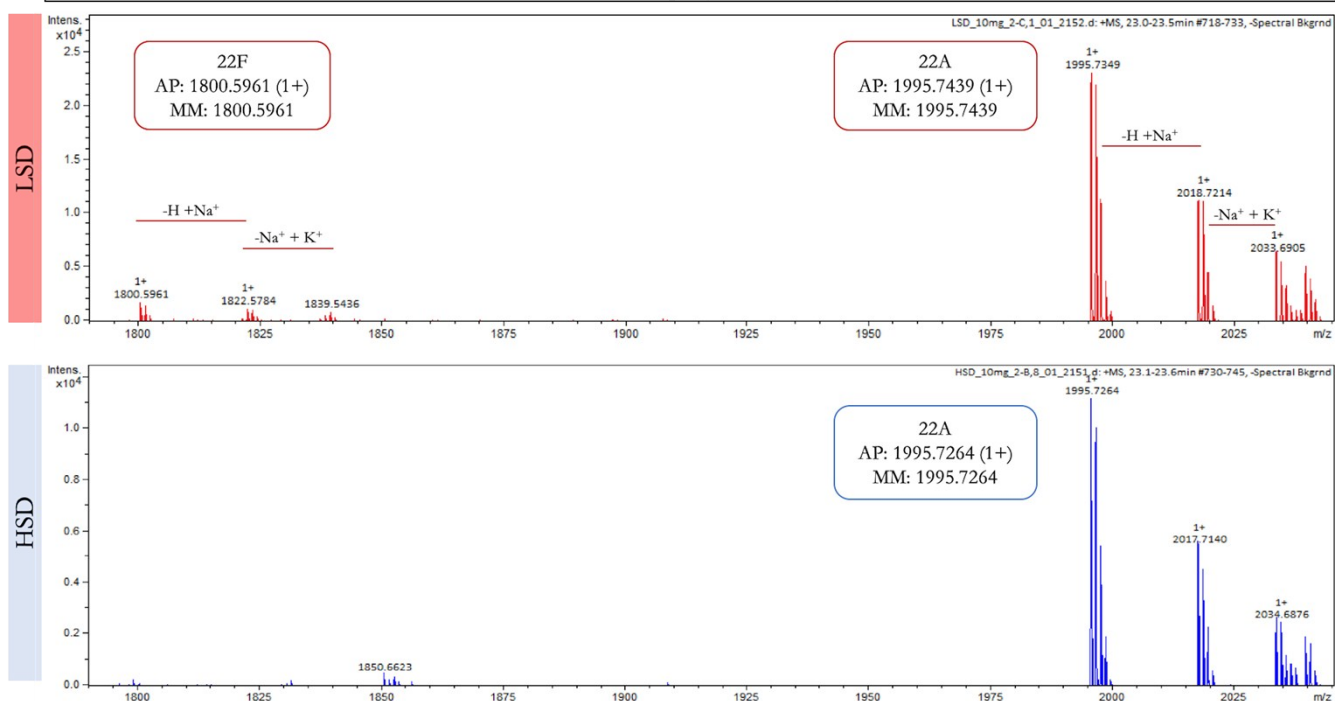


Figure S-17. MS spectra extracts exemplifying monosaccharide compositions uniquely identified by the LSD method. Numbers reported above each peak are isotopic masses. The charge state for each value is also reported; AP indicates the mass of the actual, non-deconvoluted, monoisotopic peak in the isotopic distribution (charge state is reported in brackets); MM indicates the monoisotopic mass of the deconvoluted signal. X-axis represents mass to charge ratio and Y-axis represents the absolute signal intensity. Inside each spectrum frame the following information is reported: name of the sample; MS acquisition mode (positive); start and end points of the averaged section (min); background removal type (spectral).

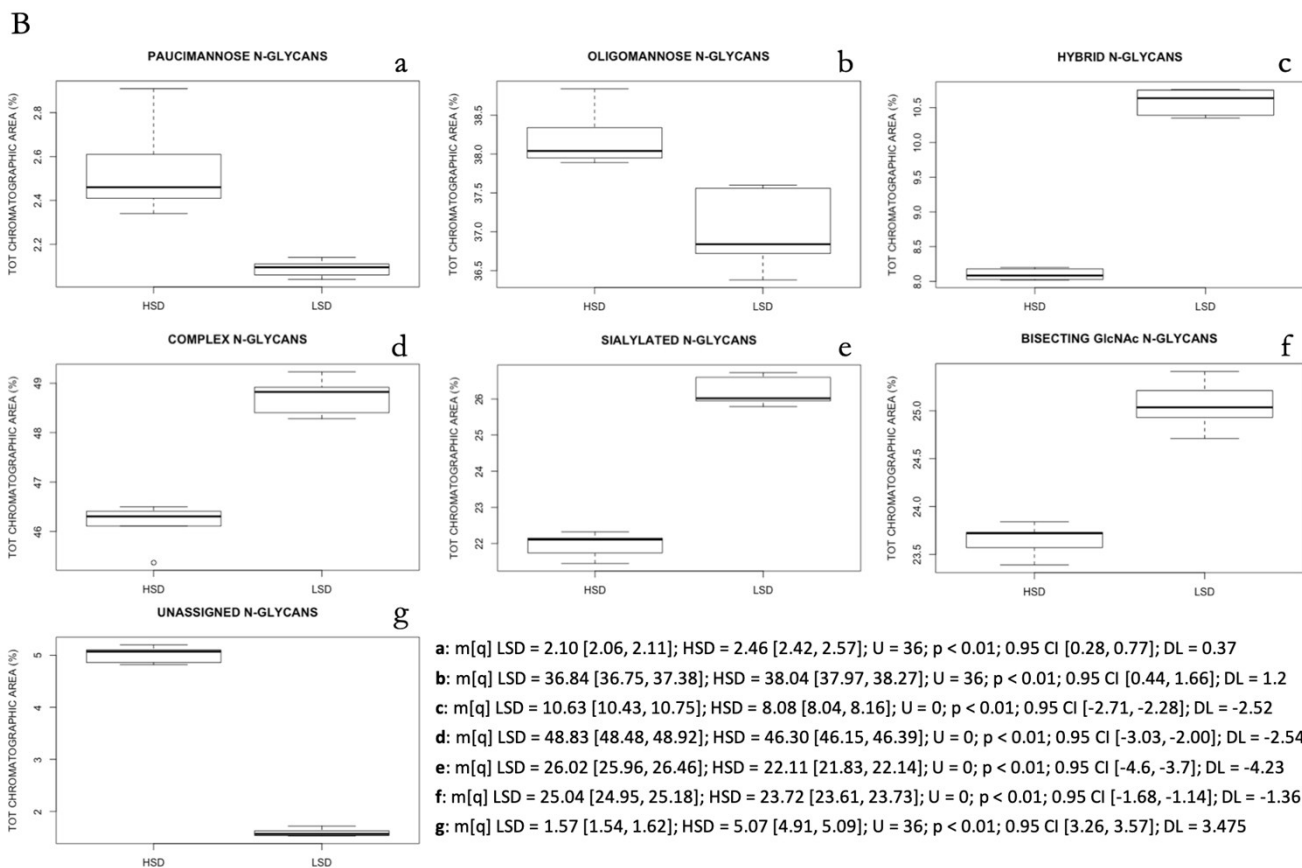
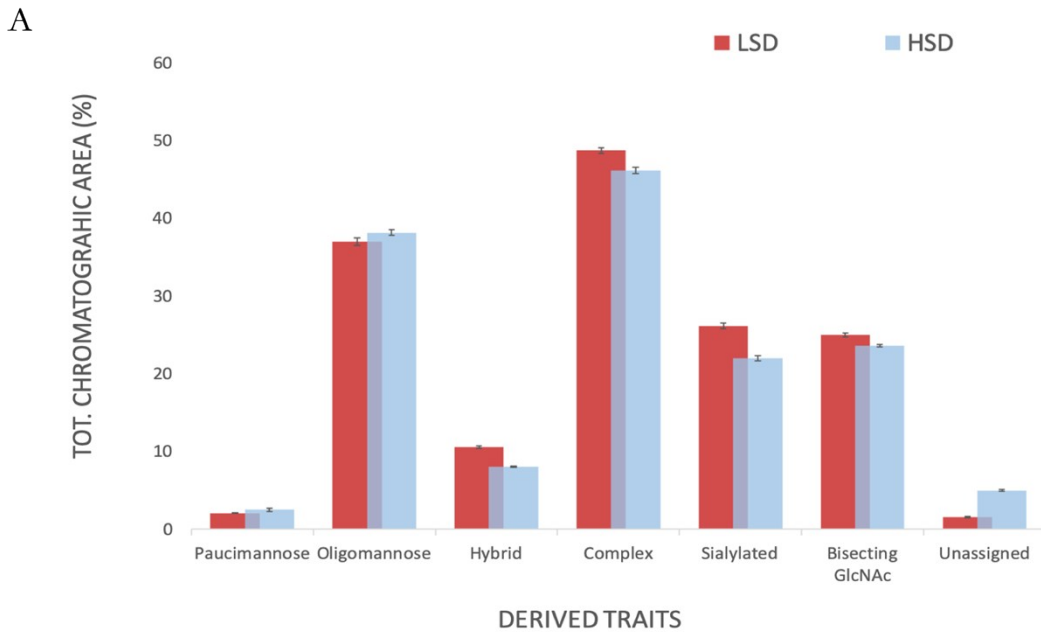


Figure S-18. Derived traits: grouping of N-glycans according to structural features for each method. The calculations for determining the derived traits are given in Supplementary Material 1: Calculation of derived traits. Only N-glycan compositions that could unambiguously be assigned to certain structural groups were included. Note that it was not possible to assign all N-glycans to structural groups due to lack of MS data to resolve potentially ambiguous compositions. **A.** The percentage of the total chromatographic area for each derived trait and method is reported in the histogram. Descriptive error bars show data spread within replicates ($n = 2$, triplicates, as done for the analysis showed in Figure S-13) as \pm SD. **B.** Box-plots indicate dispersion and skewness of the data for every derived trait comparison reported in A. The statistical analysis (Wilcoxon-Mann-Whitney, $n = 2$, triplicates) is summarized in the lower part of the image through the presentation of relevant parameters.

Supplementary material 1: Calculation of derived traits

The chromatographic sections assigned to each group are listed below for each method:

Paucimannose

LSD: 1,2,3,4.

HSD: 1,2,3,4.

Oligomannose

LSD: 7,13,14,20,22,25,26,29.

HSD: 7,13,14,15,20,25,26,29,30.

Hybrid

LSD: 11,12,15,18,23,27,28,33.

HSD: 11,18,22,27,28,33.

Complex

LSD: 5,6,8,9,10,16,17,19,21,24,30,31,32,34,35,36,37,38,40,41,42,43,44,46,47,48,49,50.

HSD: 5,6,8,9,10,17,19,21,24,31,32,34,35,36,37,40,41,42,43,44,46,47,48,49.

Sialylated

LSD: 16,30,31,32,34,35,36,37,38,41,42,43,44,46,47,48,49,50.

HSD: 22,31,32,34,35,36,37,41,42,43,44,46,47,48,49.

Bisecting GlcNAc

LSD: 3,5,8,11,12,15,17,18,19,24,28,31,32.

HSD: 3,5,8,11,17,18,19,24,31,32.

Not determined

LSD: 39,45.

HSD: 12,16,23,38,39,45,50.

Supplementary material 2: Lysate in-Solution Deglycosylation (LSD) protocol

Prepare Radioimmunoprecipitation Assay (RIPA) lysis buffer

- 25 mM Tris-HCl, pH 7.6
- 150 mM NaCl
- 1% (v/v) Igepal-CA630
- 1% (w/v) Sodium Deoxycholate
- 0.1% (w/v) SDS
- Supplemented with 1X Complete™ Mini EDTA-free Protease Inhibitor Cocktail (Sigma-Aldrich)

Solutions and reagents

- Cold lysis buffer containing protease inhibitors
- 10% (w/v) SDS
- 10% (v/v) Igepal-CA630
- 20mM NaHCO₃, pH 8.6
- Methanol
- Chloroform
- PNGase F, 10,000 U/mL (Promega)

Tissue lysis and homogenisation

- Place an empty microfuge tube on a balance and tare it
- Add tissue to tube and record its mass
- Add appropriate volume of cold lysis buffer (rule of thumb; approx. 10 µL per 1 mg of tissue for a 100 µg/µL lysate)
 - For small amounts of tissue, prepare a more dilute lysate to avoid losses in the homogenization step but use a greater volume of lysate in the methanol/chloroform extraction step
- Incubate on ice (or +4 °C) for 10 min
- Use a 1 mL syringe to thoroughly homogenize the tissue using a 20G needle
 - Despite not being tested by the authors, an alternative method (e.g. sonication) could probably be used instead of physical disruption to lyse the tissue
- Centrifuge for 20 min at room temperature at maximum velocity (12,000 g)
- Transfer supernatant to a clean 1.5 mL microfuge tube

Methanol/chloroform extraction of (glyco)proteins

- Take a volume of lysate containing the equivalent of 1-10 mg of tissue (i.e. 10-100 µL of a 100 µg/µL lysate)
 - Recommended starting amount for UPLC analysis: 50 µL of a 100 µg/µL lysate (i.e. equivalent to 5 mg of tissue)
 - Recommended starting amount for MS analysis: 100 µL of a 100 µg/µL lysate (i.e. equivalent to 10 mg of tissue)
- Add water to 200 µL
- Add 600 µL of methanol
- Add 150 µL of chloroform
- Vortex
- Add 450 µL of water
- Vortex
- Centrifuge 2 min at room temperature (maximum velocity)
- Remove and discard aqueous phase
- Add 450 µL of methanol
- Vortex
- Centrifuge 2 min at room temperature (maximum velocity)

- Remove and discard supernatant
- Dry protein pellet (approx. 5 min in vacuum centrifuge or air dry 10-15 min on bench)

Resuspension, denaturation and deglycosylation

- Reaction can be scaled up or down as required
- Prepare deglycosylation master mix

Master mix	x1	[Final]
20mM NaHCO ₃ , pH 8.6	48 µL	-
10% SDS	1.7 µL	0.35% (w/v)
β-mercaptoethanol	0.3 µL	0.60% (v/v)
Total volume	50 µL	

- Resuspend protein pellet in 50 µL deglycosylation master mix
- Vortex and briefly centrifuge samples, then denature proteins with incubation at 60 °C for 10 min
 - Do not use high temperatures for denaturation to preserve labile sialic acids
- Allow mixture to cool to room temperature (approx. 5 min on bench)
- Add 5.5 µL 10% Igepal-CA630 to each sample (final concentration 1%) to neutralize SDS
- Vortex and briefly centrifuge samples
- Add 0.5 µL PNGase F (5 units)
- Vortex and briefly centrifuge samples
- Seal tubes with parafilm to prevent evaporation and incubate at 37 °C overnight

-
- Remove parafilm and add a further 0.5 µL of PNGase F (5 units)
 - Vortex and briefly centrifuge samples
 - Seal tubes with parafilm to prevent evaporation and incubate at 37 °C overnight
-

Methanol/chloroform extraction of N-glycans

- Briefly centrifuge tubes to bring down the condensate
- Add 143.5 µL of water to bring the total volume to 200 µL
- Add 600 µL of methanol
- Add 150 µL of chloroform
- Vortex
- Add 450 µL of water
- Vortex
- Centrifuge 2 min at room temperature (maximum velocity)
- Collect the aqueous phase containing the free N-glycans in a 2 mL microfuge tube*
 - Be careful not to disturb the protein layer at the interface of the organic/aqueous phases
- Dry samples (approx. 3 hours in a vacuum centrifuge)

*Note: If you wish to recover the deglycosylated protein fraction (i.e. to analyse O-glycans), after removing the aqueous phase precipitate the protein fraction by adding 450 µL of methanol, then vortex, centrifuge 2min at room temperature (maximum velocity), and then remove and discard supernatant.

N-glycan labelling and analysis

- Resuspend N-glycans in 50 µL of water
- Continue with labelling method/analysis of choice